PHILOSOPHICAL TRANSACTIONS OF THE ROYAL SOCIETY A MATHEMATICAL, PHYSICAL & ENGINEERING SCIENCES

Steady and Unsteady Wind Loading of Buildings and Structures [and Discussion]

C. Scruton, E. W. E. Rogers, J. B. Menzies and R. S. Scorer

Phil. Trans. R. Soc. Lond. A 1971 **269**, 353-383
doi: 10.1098/rsta.1971.0038

Phil. Trans. Roy. Soc. Lond. A. **269**, 353–383 (1971) [353]
Printed in Great Britain

II. WIND EFFECTS ON BUILDINGS AND OTHER STRUCTURES

Steady and unsteady wind loading of buildings and structures

By C. Scruton and E. W. E. Rogers
Aerodynamics Division, National Physical Laboratory, Teddington

CONTENTS

Wind loads are conveniently divided into steady (time-average) loads and unsteady (time-dependent) loads. The latter arise from fluctuating forces due to turbulence as well as from self-excited aerodynamic instability. The relevant characteristics of atmospheric winds—speed profile and turbulence—and their dependence on the local terrain are briefly discussed.

For design based on steady wind loadings the design wind speed is dependent on the acceptable degree of risk. Force and pressure coefficients may be influenced by Reynolds number, surface roughness, wind characteristics and proximity to other structures. Unsteady loadings due directly to turbulence are assessed through the concept of aerodynamic admittance. Only the vortex-shedding and galloping mechanisms leading to aerodynamic instability are reviewed here, together with some design features for avoiding such excitations.

To predict the response of even conventional structures while in the design stages further information is needed on the speeds and turbulence characteristics of natural winds, especially of those over cities. Further investigations concerning the aerodynamic admittance and the aerodynamic excitation of practical structures are also needed. Research on these properties involves wind-tunnel studies in which the separate effects of intensity and scale of turbulence must be determined, and improved techniques for simulating the characteristics of natural winds in wind tunnels are required. A major difficulty in the application of these aerodynamic data to the prediction of structural response is the uncertainty in the assessment of values of the structural damping.

1. Introduction

It was late in the nineteenth century before, prompted by the Tay Bridge disaster in 1879, engineers began to study wind loads on structures and to use them as factors in engineering design. The wind loads were at that time regarded as definitive steady loads which could be applied as static loads in the structural design. In 1940 the long-span suspension bridge at Tacoma, U.S.A., collapsed dramatically following a period of torsional oscillation of the suspended roadway caused by the wind. This collapse, together with subsequent incidents of structural oscillations due to wind, demonstrated the significance of the oscillatory response of structures to wind. At first oscillatory responses caused by some form of aerodynamic instability were studied in which the unsteady wind forces involved are self-induced by the interaction of the structure with the airstream, and do not depend on unsteadiness in the approaching airstream. They may occur in both turbulent and smooth (non-turbulent) airstreams. Within the last ten years the significance of the dynamic response of flexible structures to the direct forcing action of the randomly fluctuating force associated with unsteadiness (turbulence) in the approaching wind stream has been realized. This type of wind loading is now finding a place in the appropriate clauses of some of the national Codes of Practice as an alternative to clauses based on the static wind loading concept which had been used almost exclusively hitherto. The static wind-loading approach is probably adequate for most conventional buildings, but consideration of the dynamic response is becoming more necessary as more slender and lighter structures are designed and as modern methods of fabrication tend to reduce the amount of damping inherent in the structure. In this paper the data pertinent to the three classes of wind loading referred to above are discussed. The final assessment of wind loading must relate to the most adverse wind conditions which the structure will experience during its lifetime, and this involves forecasting wind conditions far into the future. Such forecasts must be made in terms of probabilities and are thus associated with a certain degree of risk that the specified wind condition will be exceeded. Some brief comments on those wind characteristics relevant to structural design now follows.

2. Relevant characteristics of atmospheric winds

The characteristics of natural winds important in structural design are both complex and difficult to acquire; nevertheless they can be briefly described in terms of wind speed (or wind pressure) and its temporal and spatial variations.

(*a*) *Static wind loading*

For this case the loads will be based on the maximum mean wind speeds expected to occur during the design life of the structure, and these speeds will clearly depend on the averaging time (i.e. the gust period) adopted. For the pressures on external cladding and for the static stability of a building, gust periods of about 3 to 10 s have been suggested (Scruton & Newberry 1963) as the appropriate periods; such times allow both the air forces to develop and the structure to deflect. The spectrum of atmospheric turbulence extends over a very wide range of frequency but there is a gap of minimum energy centred around periods of 1 h. It is therefore convenient to express wind speeds in terms of an hourly mean speed, and to derive wind speeds for other, shorter, averaging periods by the application of a 'gust-factor' appropriate to the selected averaging period.

PHILOSOPHICAL TRANSACTIONS OF THE ROYAL SOCIETY A MATHEMATICAL, PHYSICAL & ENGINEERING SCIENCES

The speed of the wind increases with height and wind-speed data are therefore referred to the standard meteorological height of 10 m, or alternatively to the gradient height.† For the United Kingdom isopleths of maximum mean wind speed for a return period of 50 years are available (figure 1) (Shellard 1962). For strong winds a power-law variation of speed with height can be assumed, whose exponent depends on the gust period and on the nature of the terrain over which the wind is flowing.

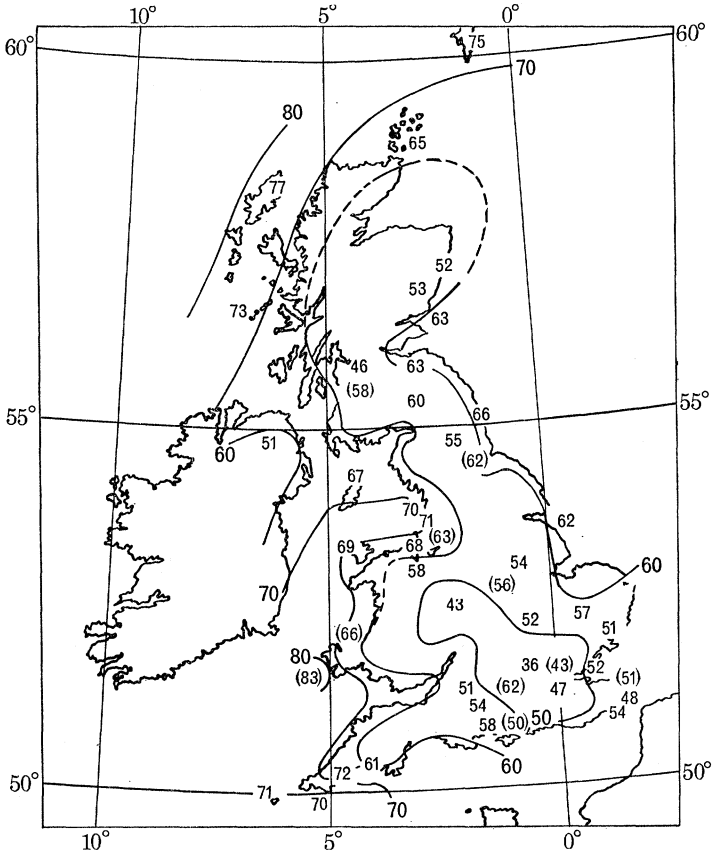

FIGURE 1. Isopleths of highest mean hourly speed (mi/h) at 33 ft (10 m) likely to be exceeded only once in 50 years (1 mi/h = 1.61 km/h).

A design wind speed for a return period of 50 years can then be written

$$\bar{V}_z^t = F_{10}^t \kappa \bar{V}_{10} (z/10)^\gamma, \tag{1}$$

where $\bar{V}_z^t$ is the maximum wind speed for period t at a height z with a return period of 50 years, κ is an adjustment factor to allow for other topographies differing from the open, level country to which figure 1 applies, z is the height, γ is the exponent for the power-law variation of the gust speed with height, $\bar{V}_{10}$ is the maximum mean hourly wind speed at height 10 m, obtained from figure 1, and F_{10}^t is the gust factor for converting mean hourly speeds at height 10 m to mean gust speeds of period t.

Values of the above quantities for three terrain categories are presented in table 1.

† The gradient height is the height at which the wind is no longer influenced by ground friction effects, but is dependent on the pressure differentials and the geostrophic forces associated with the Earth's rotation.

If τ is the return period for a wind speed V_τ, it is readily shown that the probability that V_τ is exceeded in N years is

$$P_N(>V_\tau) = 1-(1-[1/\tau])^N. \tag{2}$$

Thus using the wind data from figure 1, for which $\tau = 50$ years, and assuming a building life $N = 50$ years, the degree of risk that the design wind speed will be exceeded is $P_{50}(>V_{50}) = 0.63$. This would be considered too high a degree of risk if no reduction were to be gained from structural

TABLE 1

category	topography	κ	γ	F_{10}^t 3 s gust	F_{10}^t 10 s gust
1	*extreme exposure*—low expanses of open water and grassland	1.1	0.07	1.5	1.3
2	*medium exposure*—open country with low obstructions—trees, hedges, 2-storey buildings	1.0	0.09	1.7	1.4
3	*low exposure*—built-up areas, areas with high obstructions such as towns and cities	0.8	0.12	2.0	1.6

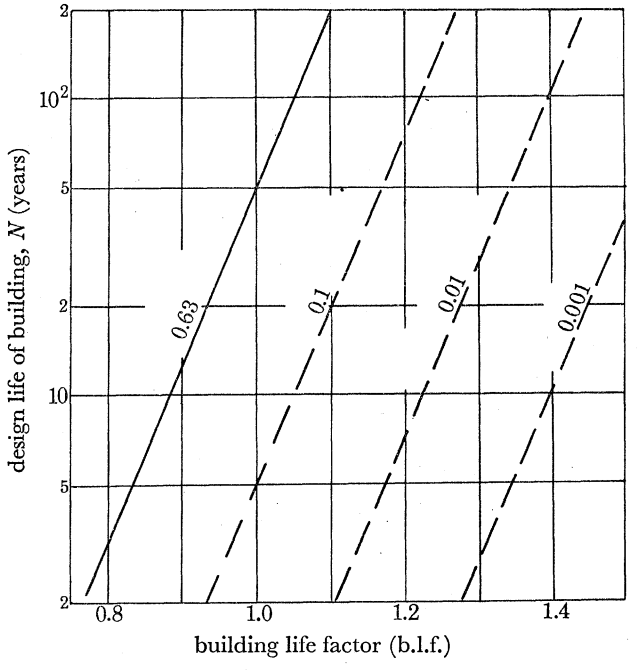

FIGURE 2. Factor for building life. Four different probabilities are shown.

safety factors. To decrease the probability requires either an increase in the design wind speed V_τ or a reduction in the design life of the structure N. A convenient method of relating design wind speed to the probability $P_N(>V_\tau)$ and building life N is through a building-life factor (b.l.f.) suggested by Mr Helliwell of the Meteorological Office. This factor is included in the 1968 Draft British Standard Code of Practice for Loading: Wind Loads (CP 3: Chap. 5),

$$\text{b.l.f.} = \frac{V_\tau}{V_s} \tag{3}$$

where V_τ is the wind speed for a return period of τ years, τ being derived from equation (2) by substituting the required degree of risk ($P_N(>V_\tau)$) and V_s is the maximum wind speed having a return period s. For the basic data in figure 1 ($S = 50$) values of b.l.f. have been computed by the Meteorological Office for different probabilities and building-life periods (see figure 2). The design wind speeds found from figure 1 and equation (1) can be adjusted by means of figure 2 to values appropriate to the specified degree of risk.

(*b*) *Dynamic wind loading*

The response of a flexible structure to the fluctuating random loading due to turbulence is computed in two parts: (1) The static deflexion due to the mean hourly wind speed; and (2) The dynamic response to the turbulence components of the wind regarded as fluctuations about the mean speed.

As in the case of static wind loading, the basic wind speed is taken as the maximum mean hourly wind at a height of 10 m (figure 1) and the variation with height is again expressed as a power law, but with an exponent α appropriate to the hourly mean. A standard normalized turbulence velocity power spectrum for the longitudinal component is

$$\frac{nS^u_{(n)}}{K\bar{V}^2_{10}} = 4\frac{X}{(2+X)^{\frac{5}{6}}}, \tag{4}$$

and this is assumed to be independent of height, wind speed and terrain roughness. In this expression n is the frequency, u is the longitudinal component of turbulence, $S^u_{(n)}$ is the power spectral density function of the longitudinal component of turbulence u, K is the surface roughness coefficient, $\bar{V}_{10}$ is the mean hourly wind speed at height 10 m and $X = n\mathscr{L}/\bar{V}_{10}$, where $\mathscr{L}$ is an arbitrary length.

When Davenport's suggested value (Davenport 1961) of $\mathscr{L} = 1200$ m is used, the above spectrum yields the variance

$$[\sigma^u]^2 = 6.7K\bar{V}^2_{10}. \tag{5}$$

TABLE 2

category	α	K
1	0.16	0.005
2	0.28	0.015
3	0.40	0.0050

On combining this with the power-law profile, the intensity of turbulence and the integral scale of turbulence at height z are given by

$$\sigma^u_z/\bar{V}_z = 2.58K(10/z)^\alpha, \tag{6}$$

$$[L^u_x]_z = 100(z/10)^\alpha \text{ metres}. \tag{7}$$

Values of α and K are given in table 2 for the three terrain categories used in table 1.

The above expressions describe the turbulence properties at a point in space. Design analyses for structures require a knowledge of the spatial correlations, and particularly of the lateral and vertical correlations of the longitudinal component u. The spatial correlation may be expressed by the coherence, based on the normalized cross-correlation spectral density function for individual wave numbers

$$\text{coherence} = \left[\frac{S^u(z, z', n/\bar{V})}{S^u(z, n/\bar{V})}\right]^2. \tag{8}$$

For vertical correlation of the longitudinal component Davenport (1967) gives the following relation showing the dependence on the wavenumber and on $\Delta_z = z - z'$

$$\sqrt{(\text{coherence})} = \exp\{-k\Delta_z(n\sqrt{\bar{V}_{10}})\}. \tag{9}$$

The coefficient k depends on the terrain. For built-up areas and open country $k = 6$ and 7.7 respectively.

3. Steady wind-load coefficients

The steady wind-load coefficients are the time-averaged load coefficients which would be used with the design wind speeds of § 2 (*a*) to obtain static wind loading and also for estimations of the loading due to the mean component of wind speed in the dynamic approach of § 2 (*b*). These force and pressure coefficients are given respectively by

$$C_{\mathrm{F}} = \frac{F}{\frac{1}{2}\rho\bar{V}^2 A}; \quad C_{\mathrm{p}} = \frac{P}{\frac{1}{2}\rho\bar{V}^2}. \tag{10}$$

Here ρ is the air density and A is some reference area.

Most of the information given in the present Codes of Practice and also in published compilations of such information quote values of these coefficients which have been found from model tests in wind tunnels. They were thus obtained with the smooth uniform airflow required for aeronautical investigations rather than the turbulent shear flows characteristic of atmospheric winds. The Reynolds number for these model tests are also considerably lower than those appropriate to full-scale conditions. It is therefore of interest to examine the influence of Reynolds number, shear profile, and turbulence on the drag and pressure coefficients of the bluff aerodynamic shapes used for buildings and structures.

The influence of Reynolds number on the drag and pressure distributions for bodies of simple sectional shape, such as the square and the circle, have been studied extensively and are well-known. Unless the body has sharp edges or protuberances which fix the position at which the airflow separates from the body, changes in the flow régime occur at some critical Reynolds number when the wake narrows and there is a consequent reduction in the drag coefficient C_D. This is illustrated in figure 3, which shows that quite a moderate rounding of the corners of a square cross-section results in a marked decrease in the drag coefficient as well as causing the coefficient to become Reynolds-number dependent. Both surface roughness and stream turbulence tend to promote transition from the subcritical to the super-critical flow régime at lower values of the Reynolds number. Figure 4 shows the very considerable effect of Reynolds number on the pressure distribution around a two-dimensional circular cylinder. The three curves are each typical of a Reynolds number range. $Re = 1.1 \times 10^5$ is a subcritical value with a laminar boundary-layer separation, a wide wake and a high drag. At $Re = 6.7 \times 10^5$ the flow is supercritical, having laminar bubble reattachments, subsequent turbulent separation, a narrow wake and a low drag. The flow illustrated for $Re = 8.4 \times 10^6$ is in the range termed by Roshko 'transcritical' when the turbulent boundary becomes established and separates over forward surfaces of the cylinder; the wake widens and the drag coefficient increases again. The Reynolds numbers appropriate for full-scale flows about buildings and structures are usually in the supercritical and transcritical ranges of Reynolds number, while most wind-tunnel measurements can be carried out only at subcritical Reynolds numbers. The problem of extrapolating wind-tunnel results to full-scale Reynolds numbers for sensitive shapes is therefore one of considerable difficulty.

PHILOSOPHICAL TRANSACTIONS OF THE ROYAL SOCIETY A MATHEMATICAL, PHYSICAL & ENGINEERING SCIENCES

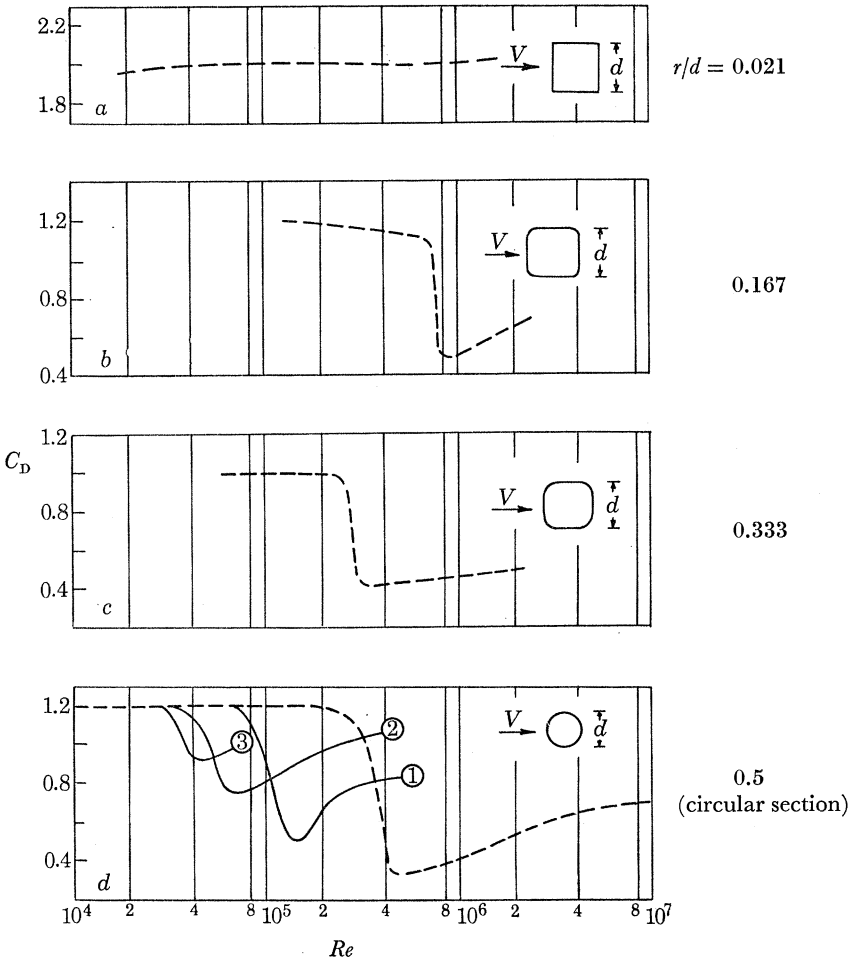

FIGURE 3. Influence of Reynolds number, corner radius, and surface roughness on the values of C_D for prisms of square section and circular cylinders (a.r. = ∞). – – –, smooth surface; ——, sanded surface. In 3*d*: (1) $k/d = 0.002$; (2) $k/d = 0.007$; (3) $k/d = 0.020$ (where k is the grain size of sand).

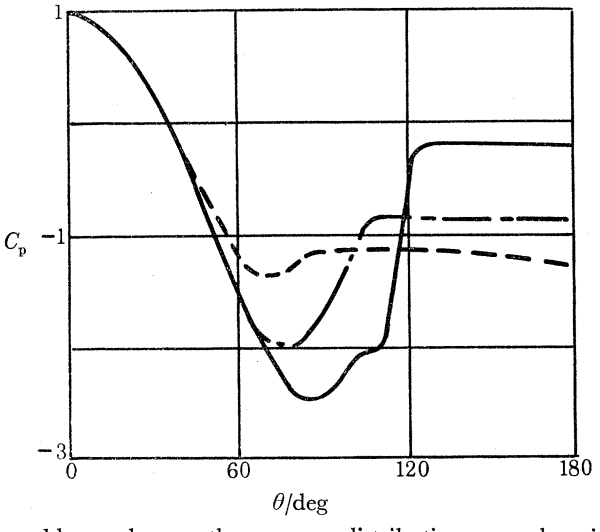

FIGURE 4. Influence of Reynolds number on the pressure distribution around a circular cylinder (a.r. = ∞). ——, $Re = 6.7 \times 10^5$ (Flachsbart); — – —, $Re = 8.4 \times 10^6$ (Roshko); – – – –, $Re = 1.1 \times 10^5$ (Fage & Falkner).

It has been suggested that structures of low aspect ratio (e.g. cooling towers) where the flow pattern may well be dominated by the flow over the top, might be insensitive to Reynolds number effects when the top is sharp-edged (i.e. not domed). Pressure distributions around the throat of a model cooling tower (Armitt 1968) for a wide range of Reynolds numbers are given in figure 5.

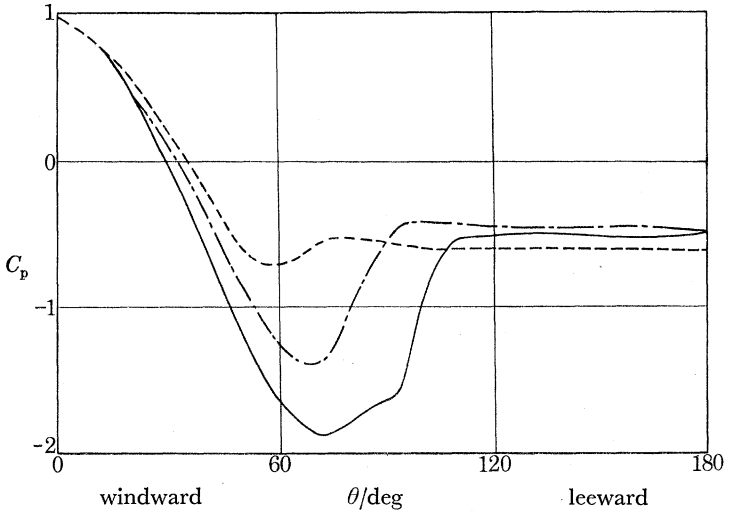

FIGURE 5. Influence of Reynolds number on the pressure distributions around the throat of a model cooling tower ----, $Re = 7.4 \times 10^4$; ——, $Re = 6.5 \times 10^6$; ——, $Re = 3.4 \times 10^5$.

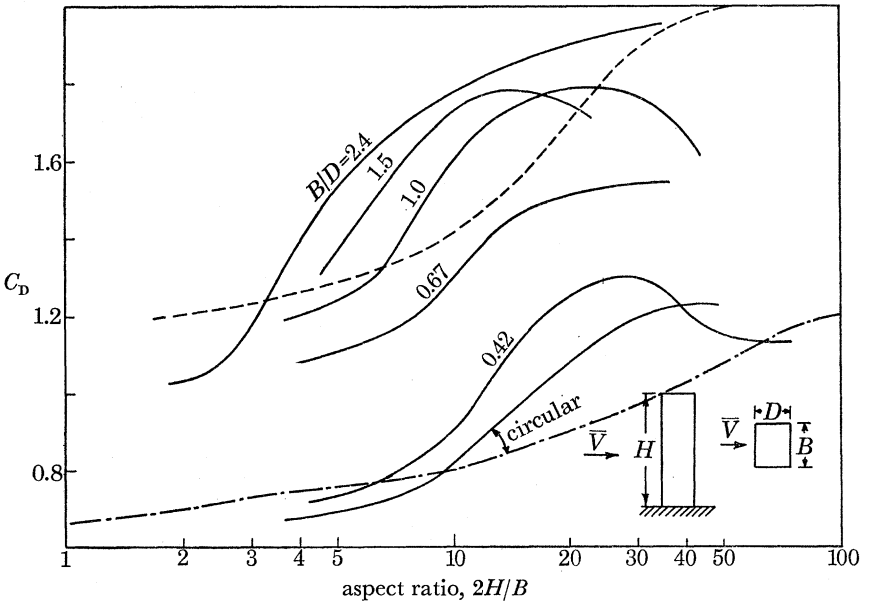

FIGURE 6. Influence of turbulence and aspect ratio on the drag coefficient of tower blocks of rectangular and circular section. ——, turbulent flow; ---- and ——, smooth flow.

The base pressure $C_{p,b}$ (i.e. the average surface pressure in the region $\theta = 180°$) shows little variation with Reynolds number and because $C_D \approx -C_{p,b}$ it can be inferred that the sectional drag coefficients for a cooling tower are not very sensitive to Reynolds number. However, the important suction (or under pressures) at the sides of the cooling tower show considerable dependence on Reynolds number.

The mean drag forces in turbulent flow must depend on both the intensity and the scales of the turbulence; the former property has a major influence on the flow over a body, especially in promoting reattachment of the separated flows, and the latter influences the spatial correlation of the forces. The mean drag coefficients of rectangular building shapes of various height/breadth ratios have been measured (Vickery 1967) in a turbulent stream of about 10 % intensity, and with ratios of the longitudinal and lateral components of turbulence to the breadth of the building (B) given by $L_x^u/B = 4$ and $L_y^u/B = 1.3$ respectively. These turbulence characteristics correspond

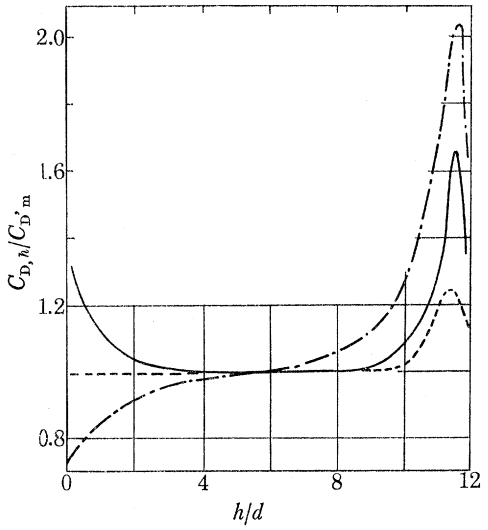

FIGURE 7. Effect of Reynolds number, turbulence, and velocity profile on the distribution of drag along a circular section chimney of height $H = 12d$. $C_{D,h}$ is the sectional drag coefficient at height h, and $C_{D,m}$ is the sectional drag coefficient at mid-height. All C_D values referred to wind speed at level of the top of the chimney.

	Re		$C_{D,m}$
——	2.7×10^6	uniform smooth flow and	0.52
		uniform turbulent flow	0.44
— — —	2.7×10^6	sheared turbulent flow ($\alpha = \frac{1}{5}$)	0.36
- - - -	0.14×10^6	uniform smooth	0.94

approximately to those of buildings in atmospheric winds. Vickery's measurements, some of which are shown in figure 6, incidentally illustrate the increase of drag coefficient with aspect ratio ($2H/B$), where H is the building height. In turbulent winds this particular increase of drag may be offset by the effect of turbulence in reducing the drag, so that for aspect ratios greater than 12 to 25 (depending on the breadth/depth ratio), the drag coefficient begins to fall as the aspect ratio rises (figure 6).

The drag is not evenly distributed along the height of a structure and the flow over the top may have a very marked effect. Measurements of the section drag coefficient (Gould, Raymer & Ponsford 1968) of model stacks of circular section showed a marked peak in the local drag coefficient occurring very close to the top of the stack (see figure 7). This peak is highest, as would be expected, with a vertical gradient of wind speed; the sectional-drag coefficient near the top is then three times as large as that near to the ground. The same distribution of sectional-drag coefficient ratio was found in smooth flows and in a turbulent flow of about 6 % intensity. In the latter case, however, the local drag coefficients for the turbulent flow are only between 80 and 90 % of those in smooth flow.

Forces and force distributions, and pressures on the cladding, can be markedly influenced by

the proximity of other structures. The shielding effect of neighbouring buildings may reduce the overall forces but may also produce an adverse distribution of these forces. An example of this is to be found in the results of an investigation (Armitt, Counihan, Milborrow & Richards 1967) to assist the inquiry into the collapse in 1965 of three of the eight cooling towers at Ferrybridge. Figure 8 exemplifies the influence grouping has on the sectional drag coefficients. Although the overall drag coefficient of a tower in the leeward row (1A) is less than that of an isolated tower,

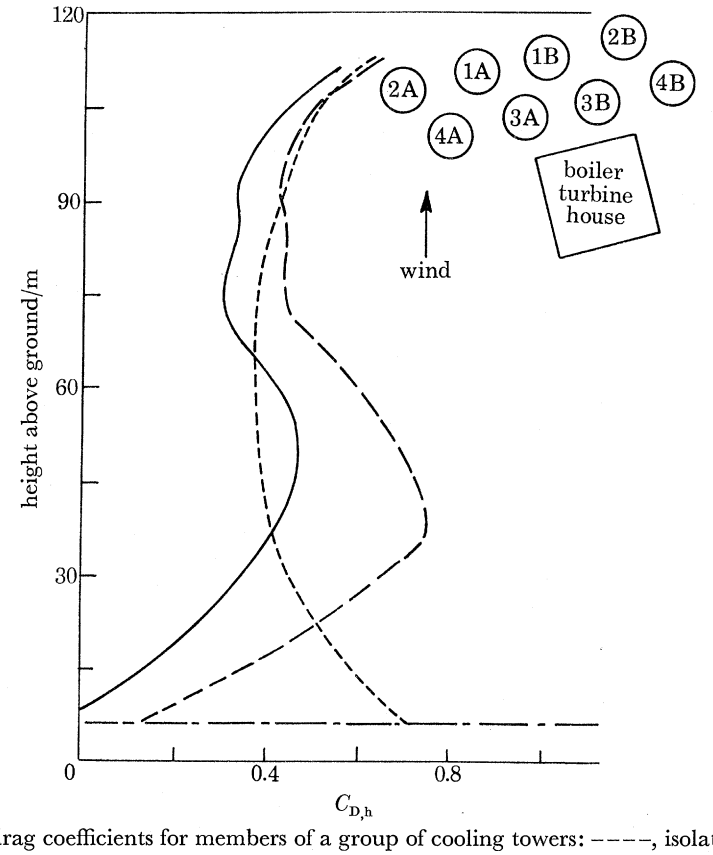

FIGURE 8. Sectional drag coefficients for members of a group of cooling towers: – – – –, isolated tower, $C_D = 0.47$; ——, tower 1A of complete model, $C_D = 0.34$; — — —, tower 3A of complete model, $C_D = 0.54$. $Re = 2.9 \times 10^6$. C_D and $C_{D,h}$ refer to average and local height diameter respectively.

or of a windward tower in the group (3A) the difference in the distributions affected the membrane stresses adversely, and of the three cases shown in figure 8 the calculated meridional stresses produced on a windward meridian are greater for tower 1A, and less for tower 3A than that for an isolated tower.

For lower buildings (houses, hangars, schools, etc.) the outward pressures due to wind on the wall cladding and roofs is the most important design consideration and a large number of model tests have been made to determine the distributions of pressure on the external surfaces (figure 9). Most of these tests, however, have been made with isolated models in a smooth uniform airstream. More recently, both model tests and measurements on actual buildings, have shown that both the magnitude and the distribution of the pressures are greatly influenced by the shear and turbulence properties of natural wind, and also by the proximity of neighbouring buildings. The most severe underpressures on a roof develop in winds directed at a corner (see figure 9); very high underpressures may develop at the windward corner and extend leeward over the windward

slope, with diminishing intensity, in two distinctly separate regions. These local regions of high underpressure are produced by two conical vortices caused by the upflow over, and separation at, the two windward roof edges. These edges are swept back relative to the wind direction. Near the

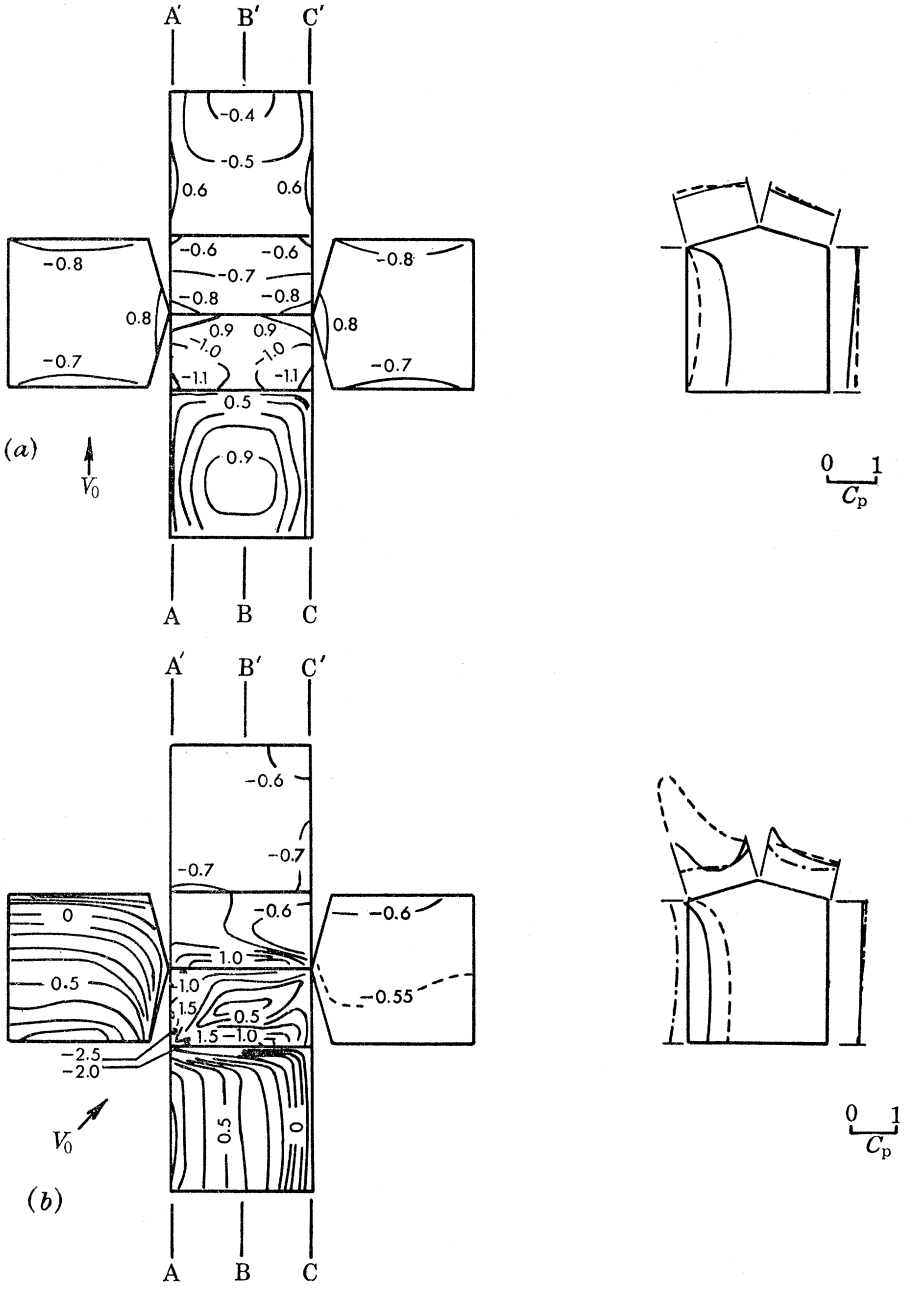

FIGURE 9. Pressure distributions over a model low-pitched roof ($\theta = 15°$) in uniform flow. (*a*) $\alpha = 0°$; (*b*) $\alpha = 45°$. – – –, A–B; ——, B–B′; —·—, C–C′.

corner the intensity of the vortex close to the roof surface is very high and so the consequent underpressure is also large. The underpressures beneath the vortices gradually decrease to leeward as the vortices rise from the surface. Fitting parapets to a flat roof effectively clears the roof of high underpressures by forcing the vortices to form well above the roof level.

The forces acting on walls, cladding, windows, etc., of a building result from the pressure differential between the pressures on the external surface and the 'internal' pressure inside the building. The internal pressure developed by wind will depend on the permeability of the walls and of the roof and on the distribution of the permeability. Where openings predominate the internal pressures will tend to take the same values as the external pressure at the position of the openings. In the extreme case of openings on one face only the internal pressure coefficient can become as large as $C_{p,i} = \pm 0.8$ according to the location of the opening; with a more even distribution, however, the internal pressure or underpressure is much reduced and for a uniform distribution $C_{p,i} = \pm 0.2$ is usually assumed. Some alleviation of the pressure differential across cladding can occasionally be gained by deliberately venting the interior to a region of underpressure on the external surfaces. For example, the ridge of a roof has a fairly high underpressure for all wind directions and wind-tunnel tests indicate that ventilators placed on the ridge are effective in reducing the uplift on the roofs even with high permeability (open windows) in the windward walls.

4. Unsteady wind loads due to turbulent fluctuations of wind speed

Methods (Davenport 1961) for calculating the dynamic response of flexible structures to the direct forcing action of the randomly fluctuating forces due to the velocity fluctuations of turbulent winds require a relation connecting the power spectral density function for velocity to that for pressure or force. For this purpose Davenport introduced a fequency-dependent transfer function $|\chi(n)|^2$, which he termed the 'aerodynamic admittance', and wrote

$$\frac{nS^f_{(n)}}{\bar{F}^2} = 4|\chi(n)|^2 \frac{nS^u_{(n)}}{\bar{V}^2}, \tag{11}$$

where $S^f_{(n)}$ is the power spectral density of the force or pressure fluctuations at frequency n, $S^u_{(n)}$ is the power spectral density of the longitudinal component of turbulence at frequency n, and $\bar{F}$ and $\bar{V}$ are the mean values of the force and the approaching wind speed.

The assessment of values for $|\chi(n)|^2$ is a topic of current research. No entirely satisfactory methods for its calculation exist and few experimental determinations have been made. For major projects wind-tunnel tests are employed which yield the deflexion spectrum from the input gust spectrum directly, and hence do not provide information on the intermediate stage of conversion from gust velocity spectrum to force spectrum.

An expression for the varying force $F(t)$ on a body in a turbulent flow of scale much larger than the body dimensions (so that the forces on the body can be assumed to be perfectly correlated) is

$$F(t) = \tfrac{1}{2}\rho V(t)\,|V(t)|\,AC_D + \rho(\mathrm{d}V(t)/\mathrm{d}t)\,(A^2/D)\,C_m, \tag{12}$$

where $F(t) = \bar{F} + f(t)$, $V(t) = \bar{V} + u(t)$, D and A are a typical body dimension and a reference area used for defining C_D, C_D is the drag coefficient, and C_m is the virtual mass coefficient.

It can readily be shown that

$$|\chi(n)|^2 = 1 + (C_m/C_D)^2\,(2\pi nD/\bar{V})^2. \tag{13}$$

It will be noted that as $n \to 0$, $|\chi(n)|^2 \to 1$. This limit can apply if the dimensions of the body are very small compared with the scale of turbulence. When this is not so, the aerodynamic admittance will be modified (reduced) by the spatial correlations of the turbulence.

For structures of finite dimensions where spatial considerations are important an analytical method for estimating the aerodynamic admittance (Vickery 1965) assumes that a solid plate normal to the flow can be treated as a lattice plate composed of a uniform grid of members of width small compared with the smallest wavelength of the velocity fluctuations of interest, and a mesh spacing large in comparison with the width of the member. With such a model it can be assumed that the presence of the plate does not influence the velocity of the airstream approaching its individual member. The expression for the admittance then becomes

$$|\chi(n)|^2 = \left\{1 + \left(\frac{C_m}{C_D}\right)^2 \left(\frac{2\pi nD}{\bar{V}}\right)^2\right\} \frac{1}{A^2} \int^A \int^A R^{uu}(a, b, n)\, \mathrm{d}A_a \mathrm{d}A_b, \tag{14}$$

where $R^{uu}(a, b, n) = S^{uu}(a, b, n)/S^u(n)$, is the normalized cross-spectral density function for forces on the small areas of the plate, $\mathrm{d}A_a$ and $\mathrm{d}A_b$ located at a and b respectively.

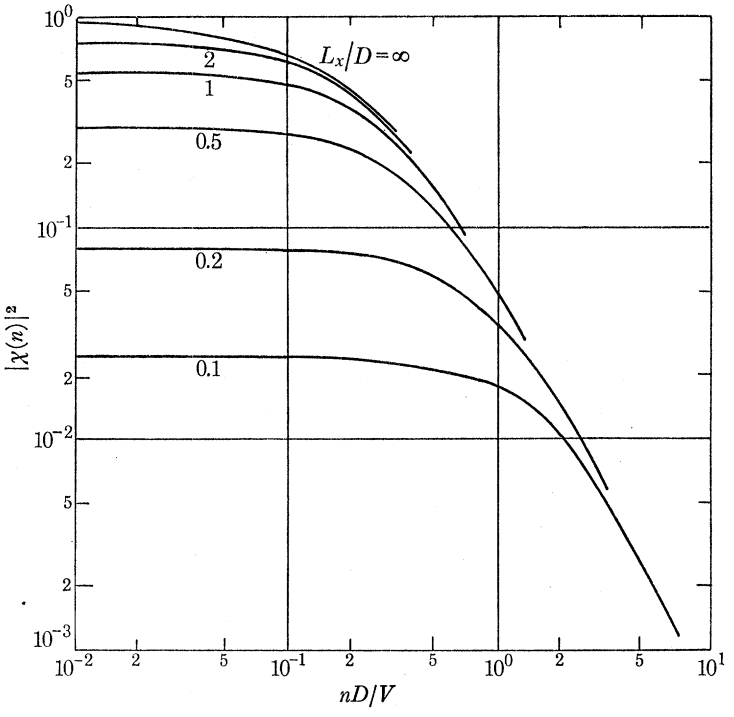

FIGURE 10. Theoretical values of $|\chi(n)|^2$ for a square lattice plate of side D.

An empirical expression for the cross-spectral density function in isotropic turbulent flow, obtained from measurements by Vickery behind a turbulence producing grid, is

$$R^{uu}(a, b, n) = \exp(-7.5\theta) \cos 1.4\pi(\theta), \tag{15}$$

where

$$\theta = \frac{r_{ab}}{2\pi L_x^u}\left[1 + \left(\frac{2\pi nL_x^u}{\bar{V}}\right)^2\right]^{\frac{1}{2}}$$

and r_{ab} is the distance between the two measuring stations a and b.

The variation of the theoretical values of $|\chi(n)|^2$ with $nD/\bar{V}$ for a lattice plate are shown on figure 10 for several values of the ratio L_x^u/D. Vickery assumed that the lattice plate theory could be applied to solid bodies and his comparisons of theoretical 'lattice' plates values with experimental values for solid flat plates and prisms showed good agreement when $L_x^u/D \approx 1$. There was little significant variation in $|\chi(n)|^2$ with the frontal shape of the prism or with the depth in the

stream direction, provided this was less than half the width. Other measurements (Bearman 1969) have confirmed this good agreement between theory and experiment for flat plates when $L_x/D > 1.5$ but indicated that the 'lattice plate' theory underestimated the experimental value when $L_x/D < 1.5$ (see figure 11). Bearman discusses this discrepancy and finds an explanation of the trend based on a turbulence distortion theory of Hunt. Much further theoretical and experimental work is required to provide a further understanding of the flow phenomena which can lead to more reliable theoretical estimates of aerodynamic admittance.

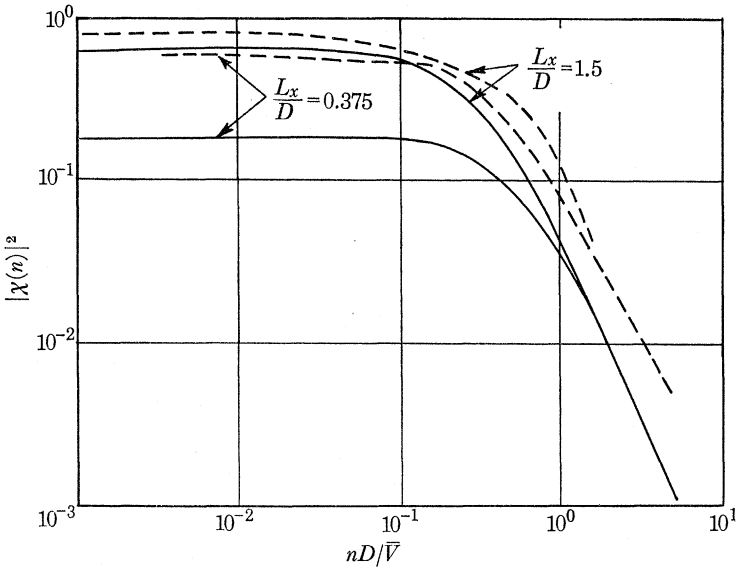

FIGURE 11. Comparison of theoretical and experimental values of the aerodynamic admittance for a flat plate. ——, theory; – – – –, experiment.

5. UNSTEADY AERODYNAMIC FORCES DUE TO AERODYNAMIC INSTABILITY

In this section the aerodynamic stability mechanisms which give rise to unsteady (usually periodic) wind forces on structures are discussed. These unsteady wind forces can be termed self-excited in that no unsteadiness is required in the approaching stream; the unsteady forces arise from the characteristics of the airflow pattern induced over a bluff structure, or by the motion of the structure. The instabilities can induce motion in a single degree of freedom, so that coupling between two degrees of freedom, as in the classical flutter mechanism, is not a necessary condition. The practical manifestation of these unsteady forces is to be found in the wind-excited oscillations of suspension bridges, in the swaying of towers, masts, stacks and tall buildings in the wind, and in the large amplitude galloping motions of transmission lines and of mast cable stays. The aerodynamic mechanisms involved include vortex-excitation, galloping excitation, stalling flutter, classical flutter, and buffeting and proximity effects.

If q is the linear displacement of the structure during oscillation, the unsteady aerodynamic force per unit length can be written in terms of the components in-phase and out-of-phase with the motion.

$$F(t) = -(K_a q + C_a \dot{q}) \tag{16}$$

and, normalizing by $\rho V^2 D$, where D is a typical dimension (e.g. width)

$$\frac{F(t)}{\rho V^2 D} = -\frac{1}{V_r^2}(k_a + i2\pi c_a)\,\eta, \tag{17}$$

where $\eta = q/D$, $\eta = \eta_0 \exp(\mathrm{i}2\pi Nt)$, $V_r = V/ND$ (the reduced velocity), $c_a = C_a/\rho ND^2$, $k_a = K_a/(\rho N^2 D^2)$, and N is the frequency of oscillation.

An alternative expression for $F(t)$, used especially for describing vortex-excitation, is based on the physical concept of a harmonic oscillation excited by the fluctuating cross-wind forces induced on a bluff body by the shedding of vortices alternately from each side.

$$F(t) = \tfrac{1}{2}\rho V^2 D c_q \cos 2\pi nt, \tag{18}$$

where c_q is the non-dimensional amplitude of the cross-wind forces and n is the frequency of the shedding of complementary pairs of vortices, and n is related to a non-dimensional Strouhal number $S = nD/\bar{V}$. However, the frequency of vortex shedding is influenced by the motion, which itself is usually invariant with wind speed so that the expression (18) is only useful when $n = N$, so that

$$F(t) = \tfrac{1}{2}\rho V^2 D c_q \cos 2\pi Nt. \tag{19}$$

This expression ignores any in-phase component of the force. It can readily be shown that c_a and c_q are related by the following

$$c_q = -\lambda c_a \eta_0 / V_r, \tag{20}$$

where λ is a constant depending on the mode of oscillation and the distribution of the cross-wind force along the length of the structure.

The above representations are adequate for systems in which the response is harmonic or nearly so. However, in some instability mechanisms the forces may contain significant random contributions spread over a broad band of frequencies. The force may then be represented by its normalized power spectral density function

$$\overline{F^2}(t) = [\tfrac{1}{2}\rho V^2 D]^2 \overline{c_q^2} \int_0^\infty S^F(n)\,\mathrm{d}n \quad \text{and} \quad \int_0^\infty S^F(n)\,\mathrm{d}n = 1. \tag{21}$$

All the above parameters expressing the unsteady aerodynamic force depend on the shape of structure, on the Reynolds number, on the reduced velocity V_r, and on the amplitude η_0. For oscillations to occur in a single-degree of freedom the aerodynamic damping C_a must be negative and be numerically equal to, or exceed, the positive damping inherent (or applied) in the structure (C_s); that is, the oscillation will be maintained, or will grow, when

$$C_a + C_s \leqslant 0.$$

It is sometimes convenient to refer these damping coefficients to the corresponding logarithmic decrement (δ_a, δ_s) of the decay of amplitude which they cause,

$$\delta_a = C_a/2MN,$$

where M is the generalized mass.

Hence $$c_a = 2M\delta_a/\rho D^2, \quad c_s = 2M\delta_s/\rho D^2.$$

The two most common causes of wind-induced oscillations of structures are vortex-excitation and galloping excitation, and in this paper discussion of the unsteady forces due to aerodynamic instability will be restricted to these causes.

(*a*) *Vortex excitation*

Figure 12 shows the idealized vortex flow past a bluff body. Periodic vortices formed alternately at the sides of the body are then shed into the wake to form a double row of vortices. The vortices in each row rotate in the same direction but with opposite directions in the two rows. As each vortex is formed and shed it gives rise not only to a small variation in the drag force in-line with

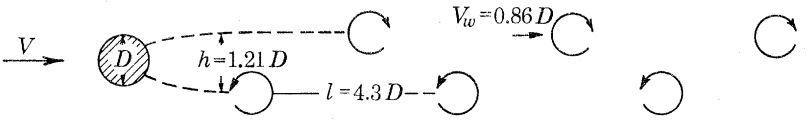

FIGURE 12. Vortex street in wake of circular cylinder V_w is the velocity of the vortex system = $0.86V$. $n = (V-0.14V_w)/4.3D = 0.20V/D$.

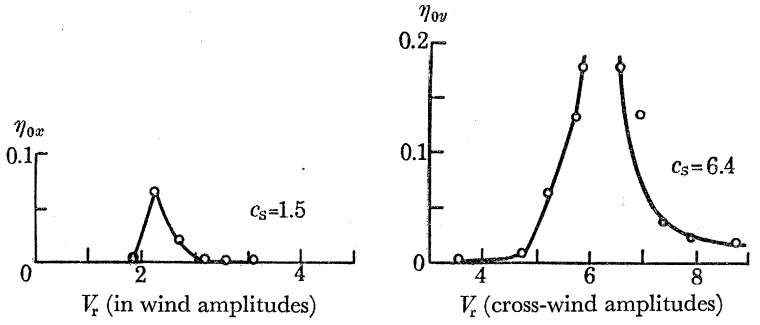

FIGURE 13. Amplitudes of a model circular stack ($L/D = 10$) oscillating in a linear mode.

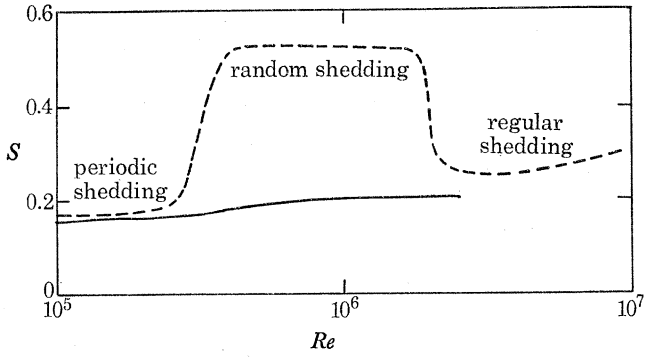

FIGURE 14. Variation of Strouhal number with Reynolds number for stationary and oscillating circular cylinders. ----, stationary cylinder; ——, model stack of circular section oscillating at peak amplitudes.

the wind but also to a more substantial force in the cross-wind, or lift, direction. This arises because of the induced change in circulation round the body. Thus an alternating force occurs on the body in the wind direction at a frequency of shedding of individual vortices and a periodic cross-wind force occurs at the frequency of shedding of complementary pairs of vortices. Maximum response of a flexible structure will therefore be expected to occur when the frequency of vortex shedding corresponds to a natural frequency of the structure, i.e. when $V = ND/S$ for cross-wind oscillations and when $V = ND/2S$ for in-wind oscillations. Figure 13 (Walshe 1968*a*, *b*) shows the amplitude response diagrams for a cantilever circular cylinder, and indicates that the excitation in the in-wind direction is very much less than that in the cross-wind direction.

The Strouhal number S is dependent on the cross-sectional shape, and at least for rounded

bodies, is sensitive to Reynolds number. It may also depend on the turbulence characteristics of the approaching airstream and on the motion itself. For a stationary circular cylinder figure 14 shows that at subcritical Reynolds numbers ($< 3 \times 10^5$) eddies are shed over a narrow band of frequencies; at super-critical values, $3 \times 10^5 < Re < 3 \times 10^6$ the energy in the eddies is more

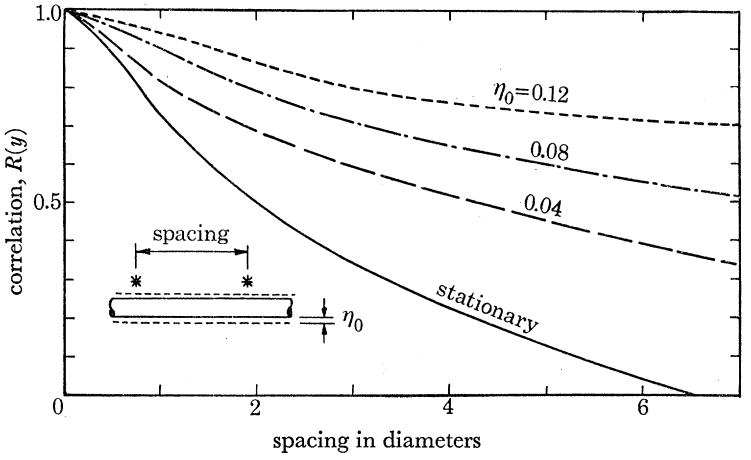

FIGURE 15. The effect of increasing the amplitude of oscillation of a circular cylinder on the correlation between the flow at two points. $Re = 0.85 \times 10^5$; $n = N$.

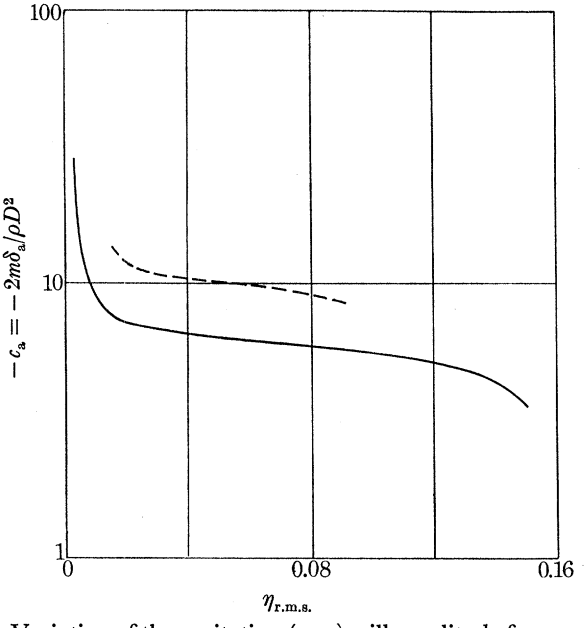

FIGURE 16. Variation of the excitation ($-c_a$) will amplitude for a model stack. $L/D = 11.5$; $V/ND = 5$. ——, $Re \simeq 6 \times 10^5$; – – – –, $Re \simeq 10^6$.

random and is spread over a much wider bandwidth of frequency. More regular periodicity recurs at about $Re = 3 \times 10^6$ with a Strouhal number of 0.28. From figure 14 it will also be seen that the effect of cylinder oscillation is to reduce the dependence of S on Reynolds number; the Strouhal number remains almost constant throughout the Reynolds number range at a value near 0.2. This result accords with the observations of oscillations on full-scale stacks which are found to oscillate at wind speeds corresponding to $S = 0.2$ for very high values of Reynolds number.

PHILOSOPHICAL TRANSACTIONS OF THE ROYAL SOCIETY A MATHEMATICAL, PHYSICAL & ENGINEERING SCIENCES

Measurements of the vortex excitation $(-c_a)$ of cylinders or prisms are often made under a 'two-dimensional' condition obtained by oscillating a cylinder of finite length transversely to the wind direction, so that the axis of the cylinder moves parallel to itself. The cylinder may be

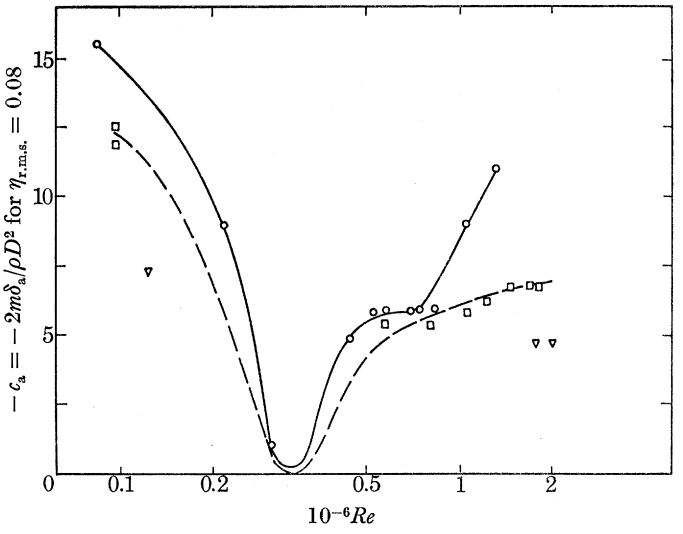

FIGURE 17. Large amplitude excitation of model stacks for a range of Reynolds number. ○——○, $L/D = 11.5$; □- - - -□, $L/D = 10$; ▽, $L/D = 8$.

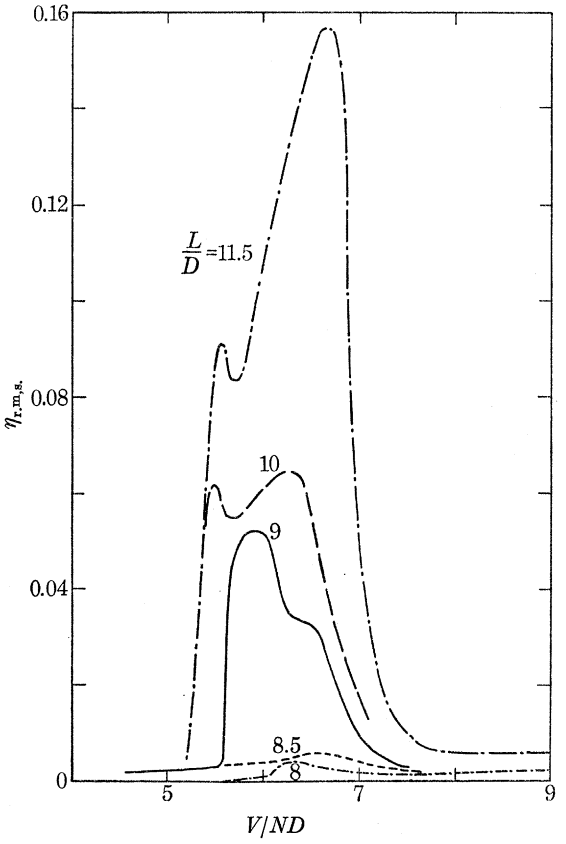

FIGURE 18. The effect of height/diameter ratio on the amplitudes of a model circular section stack at subcritical Reynolds numbers; $Re = 10^5$. $2m\delta_s/\rho D^2 = 12.0$.

provided with end-plates to prevent flow round the ends. However, although the airflow conditions may be nominally two-dimensional the flow pattern tends to form into three-dimensional cells, the axial dimension of which are measured by a correlation length defined as

$$L_y = \int_0^\infty R(y)\,\mathrm{d}y, \tag{22}$$

where the correlation coefficient $R(y)$ is defined as

$$R(y) = \frac{\overline{F_1 F_2}}{\sqrt{F_1^2}\sqrt{F_2^2}} = \frac{F_1 F_2}{[\sigma^F]^2}. \tag{23}$$

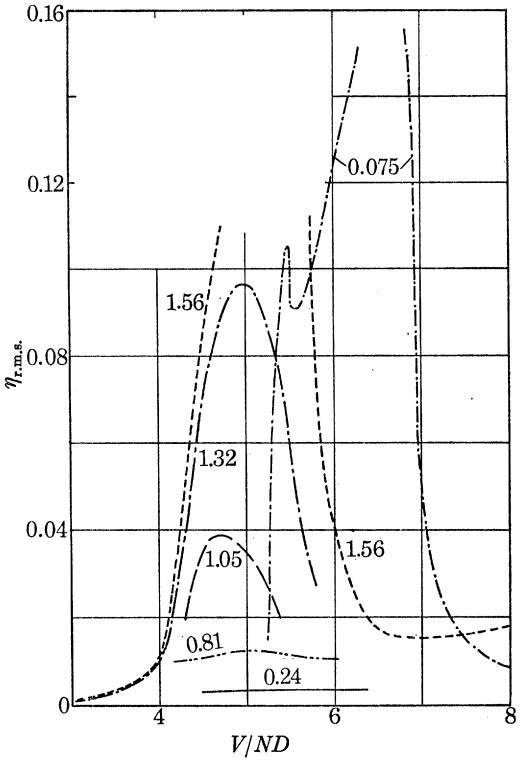

FIGURE 19. The effect of Reynolds number on the response of a circular stack of height/diameter ratio = 11.5, and structural damping $2m\delta_s/\rho D^2 = 10$. The numbers on the curves are $10^{-6}Re$ at $V/ND = 5$.

F_1 and F_2 are the forces at points 1 and 2 separated by a distance y and $[\sigma^F]^2$ the variance of the fluctuating force.

The dependence of $R(y)$ on amplitude for a cylinder oscillating in a cross-wind motion with the same amplitude along its spanwise axis (Toebes 1967) is shown in figure 15; it will be seen that the correlation length increases with the amplitude. Thus values of c_a found by assuming a uniform distribution of c_a and averaging over the length of a finite model must depend on the model length and on its mode of oscillation. The application of such values to other lengths and modes using a form of strip theory is of dubious validity, and the values should strictly be applied only to structures of similar geometry and modes to those obtaining in the tests. With this limitation in mind it is useful to look at some measurements (Wootton 1969) of the averaged excitation of cylindrical stack models oscillating in a linear bending mode. Figure 16 shows the variation of excitation with r.m.s. amplitude of oscillation. The influence of Reynolds number is shown in

figure 17; the excitation found at subcritical values reduces rapidly to almost zero at the critical Reynolds number but rises rapidly in the supercritical range. This figure also indicates the reductions in excitation with lower values of the height/diameter ratio (L/D). Both of these effects are perhaps illustrated more markedly in the response curves of figures 18 and 19.

The influence of taper of a cylindrical structure on the formation of vortices provides an interesting problem in aerodynamics. Reduction in the excitation compared with a parallel sided cylinder might be expected because of the different frequencies of vortex shedding arising from

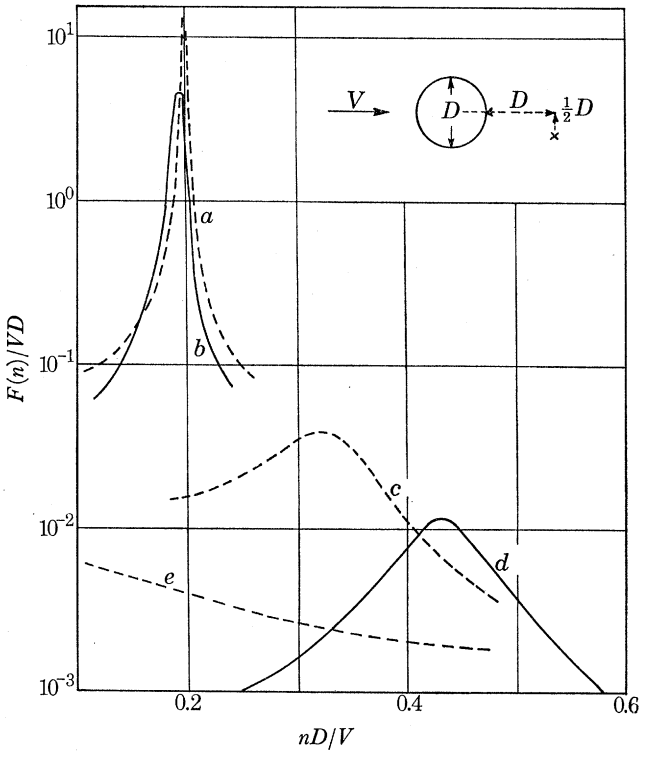

FIGURE 20. Spectra of velocity fluctuations behind a stationary cylinder in smooth and turbulent airstreams. Curve *a*, $Re = 0.26 \times 10^5$ (subcritical: turbulent stream); curve *b*, $Re = 2.2 \times 10^5$ (subcritical: smooth stream); curve *c*, $Re = 2.1 \times 10^5$ (supercritical: turbulent stream); curve *d*, $Re = 7.2 \times 10^5$ (supercritical: smooth stream); curve *e*, free stream turbulence spectrum ($\sqrt{\overline{V^2}}/V = 0.55$).

the variation of the diameter, but tests on oscillating models indicate that, at least for moderate amounts of taper, the reduction is not large. It seems that the vortex-shedding must 'lock-on' for a considerable length of the structure to the vortex-shedding frequency appropriate to a certain diameter, and that this diameter is in some way dependent on the geometry (taper ratio, length/diameter ratio) of the structure. Another consideration, with obvious similarities to the tapered cylinder in a uniform stream, is that of a parallel-sided cylinder in a stream with a wind-speed gradient.

The influence of turbulence on the frequencies of vortex-shedding from a stationary cylinder has been investigated for a limited range of Reynolds number near the critical by Bearman (Bearman 1968). The results (figure 20) indicate that when, despite the introduction of turbulence, the flow remained subcritical, the vortex-shedding remained narrow-band at $S \approx 0.2$. However, when the turbulence induced supercritical flows at lower values of the Reynolds number than in smooth flow, the shedding extended over a much wider band of frequency with

a centre frequency somewhat lower than that in the supercritical range for a smooth airstream. The authors have no information on the effects of turbulence on vortex shedding from circular cylinders in the transcritical range of Reynolds numbers ($Re > 3 \times 10^6$); it might be expected that its influence in these conditions would not be very marked.

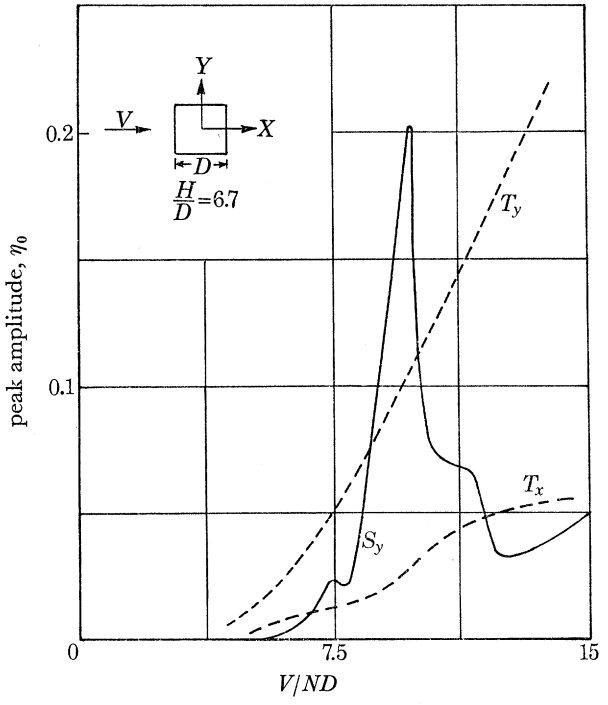

FIGURE 21. Amplitude response curves for a cantilever of square section in smooth and turbulent uniform airflows ($\delta_s = 0.07$). Curve S_y is the Y component of smooth airflow (the x component is negligible); curves T_x and T_y are the x and y components of turbulent airflow.

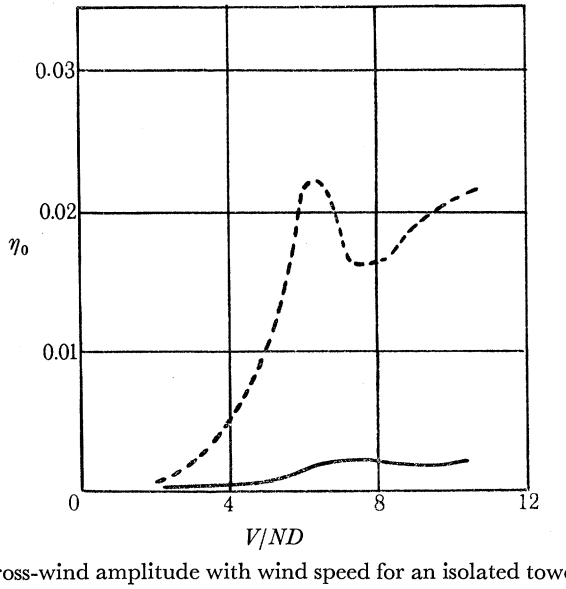

FIGURE 22. Variation of the cross-wind amplitude with wind speed for an isolated tower block of octagonal section of height/diameter ratio = 4.25, immersed in smooth and turbulent airflow ($\delta_s = 0.07$). ----, uniform turbulent flow of 11% intensity; ——, uniform smooth flow.

More significant effects of turbulence are to be found in the response curves for square-section prisms and model octagonal tower blocks oscillating in linear mode about their bases. For the square-section prism (figure 21) the introduction of turbulence of 11 % intensity changed the response from one of steady amplitude peaking at a certain wind speed to one of random amplitude steadily increasing with wind speed. The basic response is still in the cross-wind direction, and due to vortex excitation, but with an energy spectrum modified by the turbulence from a narrow-

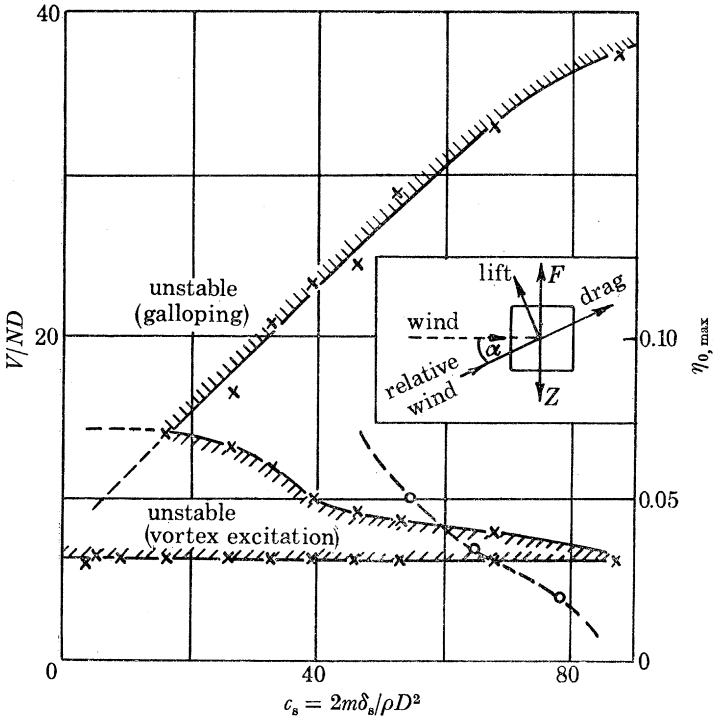

FIGURE 23. Aerodynamic stability of a long prism of square section with a face normal to the wind direction. —×—, boundary for instability; – –o– –, maximum amplitudes for the vortex-excited range ($V/ND = 6.6$).

band peaky spectrum to one extending over a wider band of frequencies and having a smaller peak intensity. A more dramatic change in the response is shown for the octagonal tower blocks in figure 22 (Whitbread & Wootton 1967).

The unsteady forces due to wind can assume higher intensities when one structure is in the wake of another. Such a situation often arises in a grouping of in-line stacks; the leeward stacks are then more prone to oscillate in wind than is the windward stack.

(*b*) *Galloping-type excitation*

Figure 23 shows a stability diagram for the transverse oscillations in wind of a long, square prism (Scruton 1960). Two regions of instability are apparent; one is ascribed to vortex-excitation and the other to galloping-excitation. Both types of instability produce motion in the cross-wind direction. The mechanism for the galloping-type excitation depends on the destabilizing character of the variation of the steady wind forces with wind inclination or with speed.

In its simplest form the excitation is due to a negative cross-wind, or 'lift', slope with incidence; an upwind produces a downward force. As the body moves across the wind direction the motion induces a relative wind inclined to the body, and when this change of incidence (α) is such as to

produce a wind force in the direction of motion, work is done on the body and instability results. It can be shown that for small amplitudes the condition for the development of an exciting force is

$$\frac{\mathrm{d}C_{\mathrm{F}}}{\mathrm{d}\alpha} = \frac{\mathrm{d}C_{\mathrm{L}}}{\mathrm{d}\alpha} + C_{\mathrm{D}} < 0.$$

Here C_{F} is the force coefficient acting in the direction of motion of the body and C_{L} and C_{D} are the usual lift and drag forces coefficients measured respectively normal and in-line with the relative direction of the wind. A simple theory (Scruton 1960) gives for the aerodynamic damping coefficient

$$c_{\mathrm{a}} = \frac{2m\delta_{\mathrm{a}}}{4\pi^2\eta_0}\int_0^{2\pi} C_{\mathrm{F}}(1+\tan^2\alpha)\cos\omega t\,\mathrm{d}(\omega t). \tag{24}$$

This can be integrated graphically or mathematically if polynomial expressions for the variation of C_{F} with α can be derived. The value of c_{a} is obviously amplitude dependent. The slope of the stability boundary of figure 23 is given by

$$-2/(\mathrm{d}C_{\mathrm{F}}/\mathrm{d}\alpha).$$

More detailed analytical investigations of the galloping excitation of rectangular prisms have been made (Parkinson 1961) and studies of the effects of wind shear and turbulence, and of the oscillation mode, have been carried out by Novak (Novak 1968, 1969).

Negative lift slopes are found for some ranges of incidence on prisms of polygonal section, and on some of the more irregular sections formed by the icing-up of transmission lines. However, icing-up is not the only cause of galloping. A stranded cable of a long-span power crossing of the Severn galloped because of the peculiar aerodynamic effects in quartering winds produced by the lay of the strands (Davis, Richards & Scriven 1963).

6. Modification and reduction of the aerodynamic excitation

When the aerodynamic excitation exceeds the structural damping, oscillations will ensue. The possible modifications to a structure which can provide freedom from wind-excited oscillations are (i) reduction in the aerodynamic excitation, (ii) increase in natural frequency if thereby the critical wind speed for any instability is raised beyond the maximum predicted wind speed for the site, and (iii) increase in the structural damping. Of these factors it is preferable to find an aerodynamic shape for which the aerodynamic excitation is reduced to an insignificant amount, or, better still, reversed in sign to become an aerodynamic damping. The most reliable way of predicting whether or not a structure will be susceptible to wind-excited oscillations is by tests of dynamically similar models in a wind tunnel. The aerodynamic shape of these models may then be modified until aerodynamic stability is achieved. This method is used in the design of long-span bridges. There may not be the same freedom to modify the shape in the case of other structures such as tall tower blocks or chimney stacks, but it may be possible to incorporate devices which reduce the excitation. These devices usually operate by either reducing the strength of the vortices formed in the wake, or by breaking up the continuity of the airflow pattern so that the unsteady forces are poorly correlated along the length of the structure. Perforating the shell of a structure so that air can pass through the shell and into the wake is effective in reducing the aerodynamic excitation. This method has been successfully applied to overcome the problem of breakage, through vortex-excited oscillations, of anti-corrosion anodes in cooling-water ducts, and model tests suggest that perforating the outer supporting shell over a short length of the top would

PHILOSOPHICAL TRANSACTIONS OF THE ROYAL SOCIETY A MATHEMATICAL, PHYSICAL & ENGINEERING SCIENCES

effectively stabilize multi-flue chimney stacks (Vickery & Walshe 1964). Such perforations have been used to avoid both vortex and galloping excitation of square-section towers.

The helical strake device (figure 24) (Scruton & Walshe 1957; Scruton 1963) has been successfully fitted on stacks and cylindrical masts. The optimum configuration for this device is a 3-start strake system with thin rectangular strakes of height $0.10D$ to $0.12D$ and would with a helix pitch of about $5D$. They are applied near the antinodes; for stacks which would oscillate in a fundamental

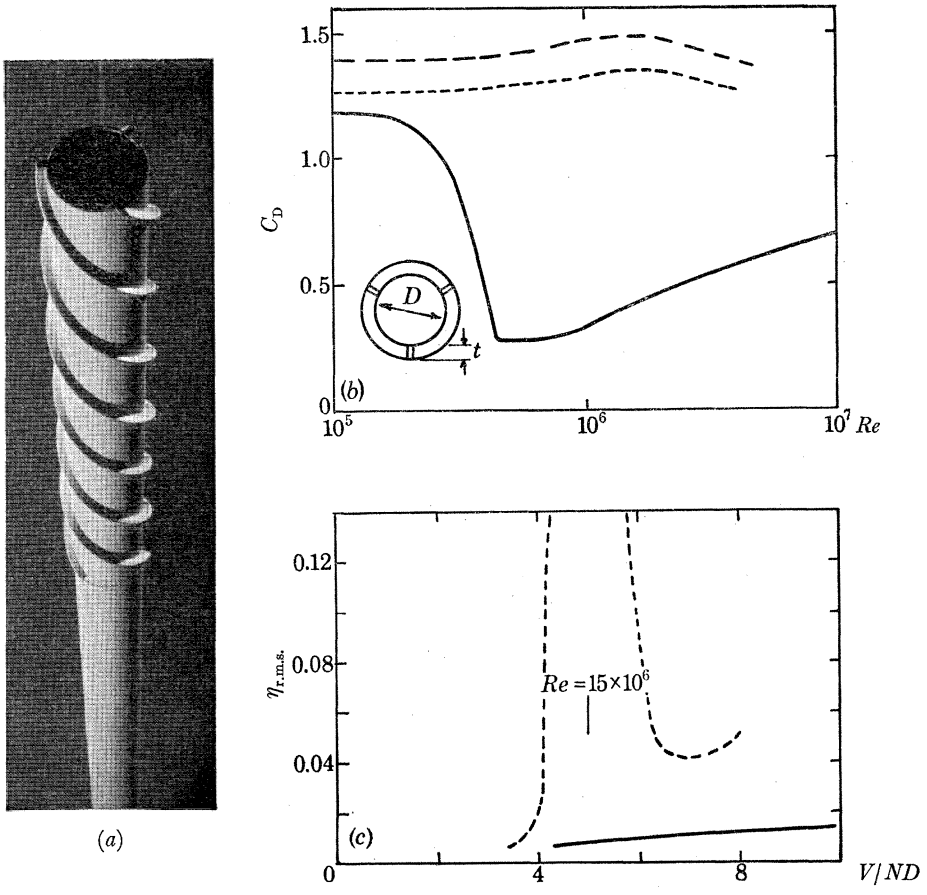

FIGURE 24. (*a*) A model straked stack. (*b*) The effect of Reynolds number on the drag coefficient of a plain straked circular cylinder. ——, plain cylinder; — — —, $t/D = 0.012$ and – – – –, $t/D = 0.006$ (cylinders with strakes). $C_D = D/\frac{1}{2}\rho V^2 DL$. (*c*) The responses of a model stack at high Reynolds numbers without and with strakes fitted over upper 30 % of stack.

cantilever mode it is usually only necessary to apply the device to the top third of the chimney. An alternative to the strake device is the perforated shroud (figure 25*a*) (Walshe 1968*b*). This consists of a perforated cylindrical shell separated from the cylinder surface by a gap. A gap width of $0.12D$ and an open area of 20 to 30 % is very effective. Like other anti-excitation devices shrouds need be fitted only near the anti-nodes.

7. FUTURE RESEARCH

With present-day trends in the design and fabrication of buildings and structures, the accurate assessment of both steady and unsteady wind loading is becoming of vital and sometimes of critical importance. Because of the random nature of atmospheric winds, and the unsteady

character of the airflow around aerodynamically bluff structural shapes, future developments in the assessments of these loads are expected to involve statistical approaches to an increasing extent. This will necessarily involve extending present efforts to determine the structure of wind

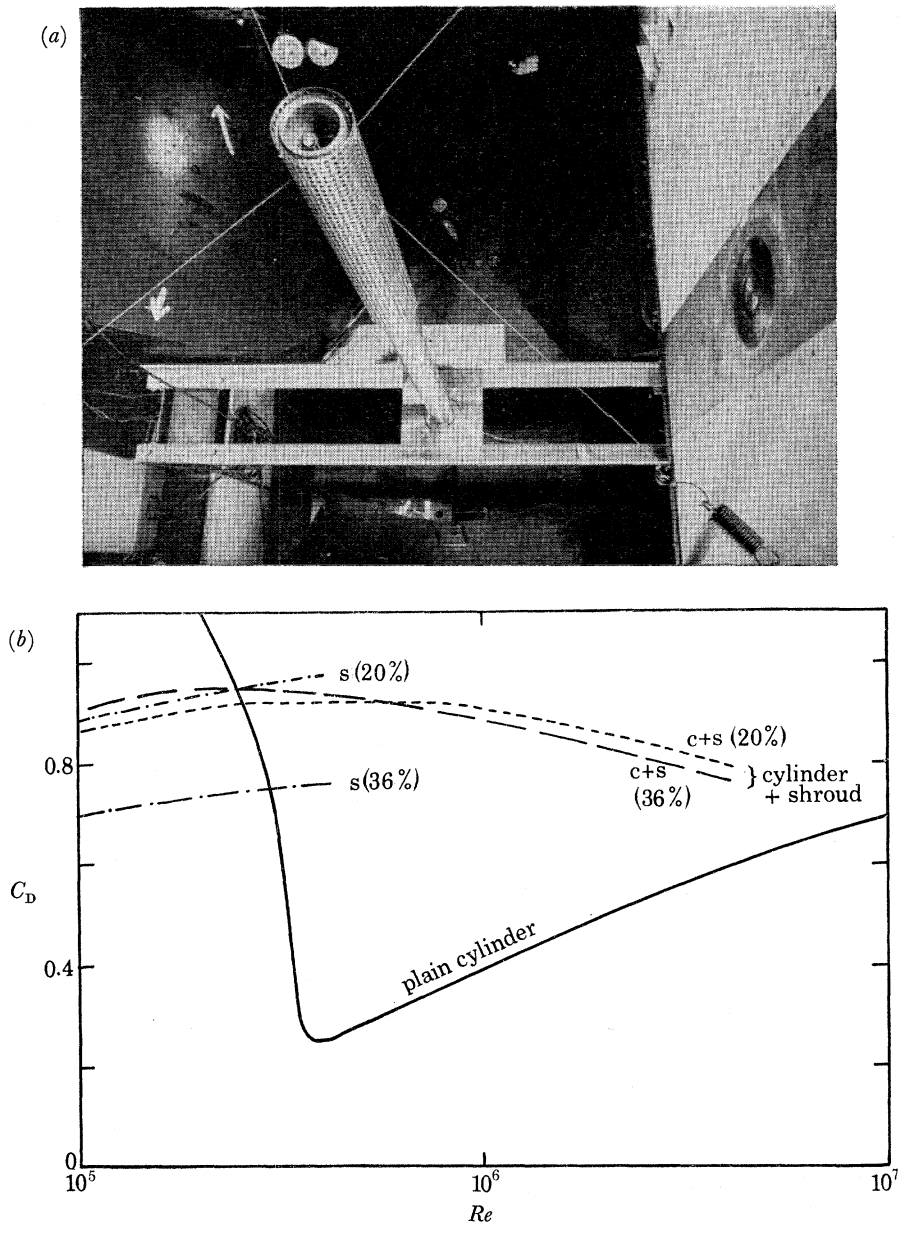

FIGURE 25. (*a*) A model shrouded stack. (*b*) The variation of drag with Reynolds number for a shrouded cylinder, shroud diameter/cylinder diameter = 1.23. *s*, shroud only; *c* + *s*, cylinder plus shroud. The percentages are the open ratios of the shrouds.

(shear, turbulence, spatial coherences) in open country and to gain similar information above urban developments and city centres.

Many of the data on steady wind loads and pressures now available come from wind-tunnel tests on models in which no attempt was made to simulate the characteristics of atmospheric winds or to examine the influence of neighbouring buildings or obstructions. Improvements to these

data can be made by investigations carried out in wind tunnels with atmospheric wind simulation. Until experimental and theoretical research on the flows around bluff bodies in both smooth uniform and in atmospheric shear flows yields a more basic understanding of the problems associated with estimations of aerodynamic admittance and aerodynamic excitation, immediate requirements for design information on unsteady wind forces must be obtained from more *ad hoc* investigations, some of which may be directed towards providing this information for simple idealized structural shapes.

This paper is published by permission of the National Physical Laboratory.

Nomenclature

A	area
B	breadth of building
a.r.	aspect ratio—length/breadth
C_F, C, C_D, etc.	non-dimensional coefficients of aerodynamic force, pressure and drag
C_m	virtual mass coefficient
D	diameter, width of body
f	time dependent component of wind force in turbulent winds
F	wind force, *also* gust factor (subscripts refer to height, and superscripts to period of time)
k	coefficient defining the coherence (see equation (9))
K	surface roughness coefficient
$L_x^u L_y^u$	respectively the longitudinal and lateral integral scale of the longitudinal component of turbulence
C_a, C_s	coefficient of velocity of motion yielding aerodynamic and structural damping forces respectively
c_a, c_s	non-dimensional forms of C_a, C_s
c_q	non-dimensional amplitude of the cross-wind forces due to vortex-shedding
K_a, K_s	coefficient of displacement yielding aerodynamic and structural (stiffness) restoring forces respectively
k_a, k_s	non-dimensional forms of K_a, K_s
M	generalized mass per unit length of structure
n	frequency of velocity fluctuations in turbulent winds, *also* frequency of shedding of complementary pairs of vortices behind a bluff body
N	natural frequency (Hz), *also* building life (years)
P	pressure difference, *also* probability
q	linear displacement of structure
r_{ab}	distance between two points a and b
$R^{uu}(a, b, n)$	normalized cross-spectral density function $= S^{uu}(a, b, n)/S^u(n)$
$Re = \bar{V}D/\nu$	the Reynolds number
$S = nD/\bar{V}$	the Strouhal number
t	time
u	along wind (longitudinal) component of velocity fluctuations in turbulent winds
V	wind speed. $\bar{V}$ denotes an average, subscripts denote height and superscripts denote period of time

$V_r = \bar{V}/ND$	the reduced velocity
$X = n\mathscr{L}/\bar{V}_{10}$	where $\mathscr{L}$ is an arbitrary length
z	height above ground
α	exponent of the power law variation of the mean hourly wind speed with height, *also* incidence
γ	exponent of the power law variation of the short duration gust speed with height
$\eta = q/D$	non-dimensional displacement
δ_a, δ_s	the logarithmic decrement of amplitudes of oscillations due to aerodynamic and structural damping respectively
κ	an adjustment factor to wind speed to allow for different topographies
ν	kinematic viscosity of air
ρ	air density
σ	standard deviation of a quantity denoted by the superscript
τ	time, years
$\lvert\chi(n)\rvert^2$	aerodynamic admittance
ω	circular frequency

References (Scruton & Rogers)

Armitt, J., Counihan, J., Milborrow, D.J. & Richards, D.J.W. 1967 C.E.R.L. Laboratory Report, no. RD/L/R/1430.

Armitt, J. 1968 *Proc. Symp. Wind Effects on Buildings and Structures*. Loughborough: Loughborough University of Technology.

Bearman, P.W. 1968 N.P.L. Aero Report 1257.

Bearman, P.W. 1969 N.P.L. Aero Report 1296.

Davenport, A.G. 1961 *Proc. Instn civ. Engrs* **19**, 449–472.

Davenport, A.G. 1967 *Proc. Int. Res. Seminar. Wind Effects on Buildings and Structures*. Toronto: University of Toronto Press.

Davis, D.A., Richards, D.J.W. & Scriven, R.A. 1963 *Proc. Instn Elect. Engineers* **110**, 205–220.

Gould, R.W.F., Raymer, W.G. & Ponsford, P.J. 1968 *Proc. Symp. Wind Effects on Buildings and Structures*. Loughborough: Loughborough University of Technology.

Novak, M. 1968, 1969 University of Western Ontario Engineering Science Research Report BLWT-3-6-8, BLWT-7-68 and BLWT-6-69.

Parkinson, A.G. 1961 *Trans ASME*; *J. appl. Mech.* **28**, 252–258.

Scruton, C. 1960 AGARD Report 309.

Scruton, C. 1963 N.P.L. Aero Note 1012.

Scruton, C. & Newberry, C.W. 1963 *Proc. Instn civ. Engrs* **25**, 97–126.

Scruton, C. & Walshe, D.E.J. 1957 N.P.L. Aero Report 335.

Shellard, H.C. 1962 *Met. Mag.* **91**, 39–47.

Toebes, G.H. 1967 *Proc. Int. Res. Seminar, Wind Effects on Buildings and Structures*. Toronto: University of Toronto Press.

Vickery, B.J. 1965 N.P.L. Aero Report 1143.

Vickery, B.J. 1967 University of Western Ontario Engineering Science Research Report BLWT-4-67.

Vickery, B.J. & Walshe, D.E.J. 1964 N.P.L. Aero Report 1132.

Walshe, D.E.J. 1968*a* N.P.L. Aero Report 1227.

Walshe, D.E.J. 1968*b* N.P.L. Aero Report 1263; also *Proc. Symp. Wind Effects on Buildings and Structures*. Loughborough: Loughborough University of Technology.

Whitbread, R.E. & Wootton, L.R. 1967 N.P.L. Aero Special Report 002.

Wootton, L.R. 1969 *Proc. Instn civ. Engrs* **43**, 573–598.

PHILOSOPHICAL TRANSACTIONS OF THE ROYAL SOCIETY A MATHEMATICAL, PHYSICAL & ENGINEERING SCIENCES

Discussion

DR J. B. MENZIES (*Building Research Station*)

I would like to describe briefly some work recently started at the Building Research Station and to discuss the way in which I think this work will help research in building aerodynamics generally to provide information that architects and structural engineers want.

It is at the design stage that the architect or engineer wishes to know the effect of wind on his buildings and, conversely, the effect of his buildings on the wind. At this stage the only practicable tool which can be used to provide the information required is the wind tunnel. But as Dr Kerensky

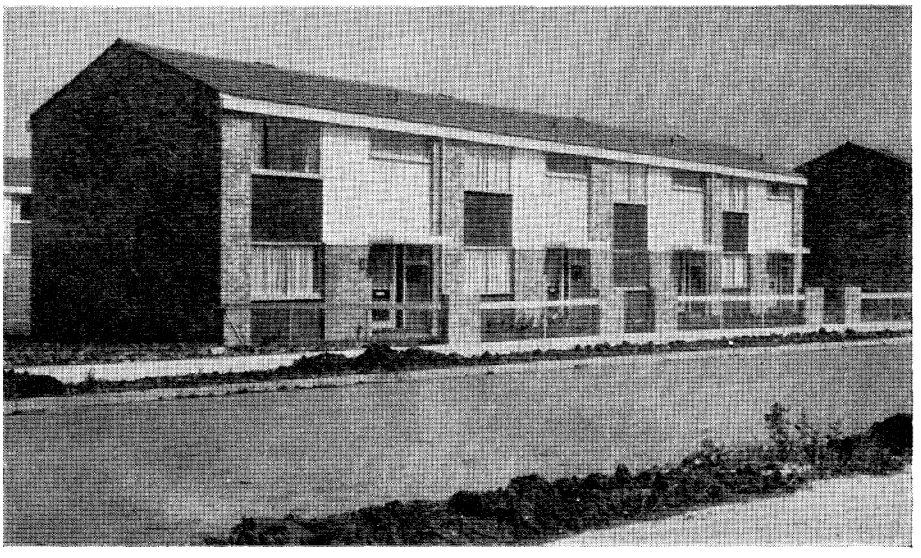

FIGURE 26

said this morning, it is necessary for the wind tunnel to be proved as an accurate means of predicting wind forces, pressures and velocities which will occur in the full-scale situation. Having proved the tool it can then be used with confidence to provide information on an *ad hoc* basis for specific building projects or, more important, to provide comprehensive information on the wind effects to be expected in a wide range of urban situations. I agree with Dr Rogers that improved techniques of simulating the natural wind in tunnels are required and I feel that one of the most important tasks now facing building aerodynamicists in improving techniques is to show that accurate predictions can be made. To do this it is vital that measurements are made on the full-scale for comparison.

It was because of doubt on the accuracy of tunnel predictions of wind forces on tall buildings in cities that the Building Research Station made measurements of wind pressure on several tall buildings in Central London. Part of the problem in using wind tunnels here was that the speed and turbulence characteristics of natural winds over cities were not known so that it was not possible to determine what were the appropriate values of speed and turbulence characteristics to model in the tunnel. The Building Research Station work on tall buildings on the full-scale has provided some information here, but more is needed if accurate predictions are to be made in the design stage. The Building Research Station work on tall buildings has, nevertheless, given us a much better idea of the wind forces on buildings which extend some distance above their neighbours. During the past year we have turned our attention to the case of a building which

has about the same height as its neighbours and have commenced work on an experiment on full-scale low-rise buildings.

Mr Lawson will be giving an outline of some aspects of this experiment in Session III (this volume, p. 493) and I would like now to anticipate what he is going to say and to add a little more background. We have chosen to study wind effects on and around two-story pitched roof dwellings (figure 26). These buildings have a roof pitch of $22\frac{1}{2}°$ and are arranged in an estate in parallel terraces about 18 m apart. The estate is situated on the southwest side of Aylesbury and there is open country to the southwest. The terraces run approximately northwest to southeast

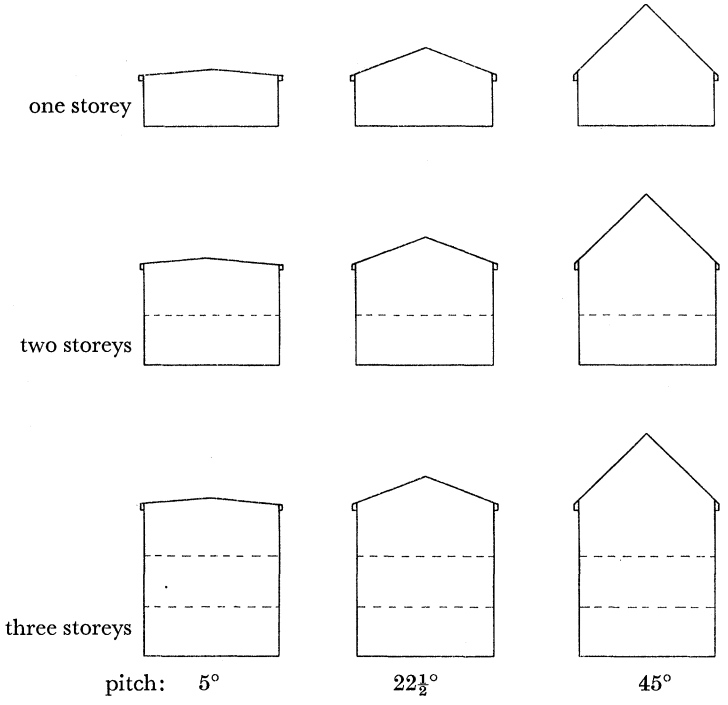

FIGURE 27. Experimental building at Aylesbury—some alternative shapes.

and thus, the prevailing wind will traverse across them. On the open ground an experimental building will be situated. This building is about the size of a semi-detached house and it is being designed so that its shape can be varied as shown in figure 27. It will be possible to construct this building with one, two or three storeys and to adjust the roof pitch to any angle between 5° and 45°. Figure 28 shows a perspective view of the site. Measurements will be made of wind pressures on the walls and roofs of seven of the houses in the estate and of wind pressures on the walls of the experimental building. On the experimental building measurements will also be made of the overall wind forces on the roof and the whole structure. Some information on the interaction between wind and snow loads on this building may also be obtained. Wind velocities will be measured at heights of 3, 5 and 10 m on an anemometer mast near to the experimental building and velocities will also be measured between the houses in the estate using a mobile anemometer mast. The measurements of velocities between houses in the estate and the related velocities over nearby open country will be extended to other estates where the planform and housing density are different. This experiment will provide, I hope, an insight into the actual wind effects on and around low-rise buildings of between one and three storeys in height with roof pitches up to 45°.

In particular it will show the differences between wind loadings on buildings situated in an exposed position on the edge of an estate and buildings sheltered from the wind within an estate.

Although this experiment will require a considerable effort, it will involve only a relatively small range of possible low-rise building shapes, densities and planforms. Having completed it and obtained good agreement in the wind tunnel, the quickest way of extending the range will be by a series of wind tunnel studies. From these studies generalized charts could be derived from which designers can assess wind loads and velocities at the design stage.

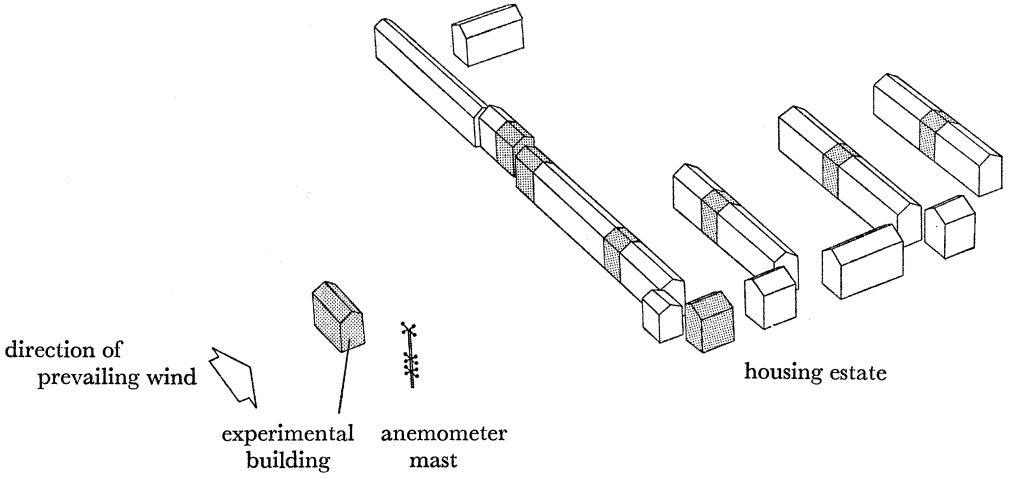

FIGURE 28. Low-rise buildings at Aylesbury.

When the building aerodynamicist has done his work there will be problems for architects and engineers in using the knowledge gained. For example, is it practicable for buildings in exposed positions on the edges of estates to be designed to withstand greater wind forces than buildings in sheltered positions within an estate supposing that the difference in wind forces is found to be relatively great? Or putting the problem in another form, can lower wind forces be used in the design of sheltered buildings when the shelter may be removed by demolition in later years? Another question, is what are the acceptable wind conditions around buildings which architects should try to achieve? These are some of the questions which must be resolved before full use can be made of aerodynamics research on groups of building.

R. S. SCORER (*Department of Mathematics, Imperial College, London*)

There is a danger of error in assuming that any sample of wind gustiness is representative because there are many different kinds of gustiness, with different geometrical configurations of motion, in the air. In particular the motion can consist of a series of fairly sharply defined gusts of cooler air, which C. S. Durst, in his memoir of about 35 years ago, described as similar to the cellular convection pattern in a viscous liquid with a wind flowing across the top. He made this analogy from measurements on the airship field at Cardington in weather with strong thermal convection and cumulus cloud. The gusts are much more pronounced when they are produced by downdrafts from showers, and in the lowest 100 m or so the gust front has an extensive part which is nearly vertical.

These small cold fronts are not properly represented by the k^{-2} spectrum which would emerge from a Fourier analysis, and they cannot be reconstituted in a wind tunnel because the density difference is essential for their persistence.

It is quite specious to argue that if the spectrum is represented by wind tunnel turbulence, and tests made on models or calculations done on a computer, satisfactory answers can be obtained, because the sophistication of the tests or computations is made phoney by the very crude safety factors that are necessarily incorporated in any design.

If the purposes of wind tunnel tests is to observe the motion of pollution in the building wake, the effects of these gusts, whose fronts might sometimes be at an azimuth other than 90° from the mean wind direction, will not be represented, and there is no satisfactory substitute for the observation of the effects in the full scale.

PHILOSOPHICAL TRANSACTIONS OF THE ROYAL SOCIETY A MATHEMATICAL, PHYSICAL & ENGINEERING SCIENCES

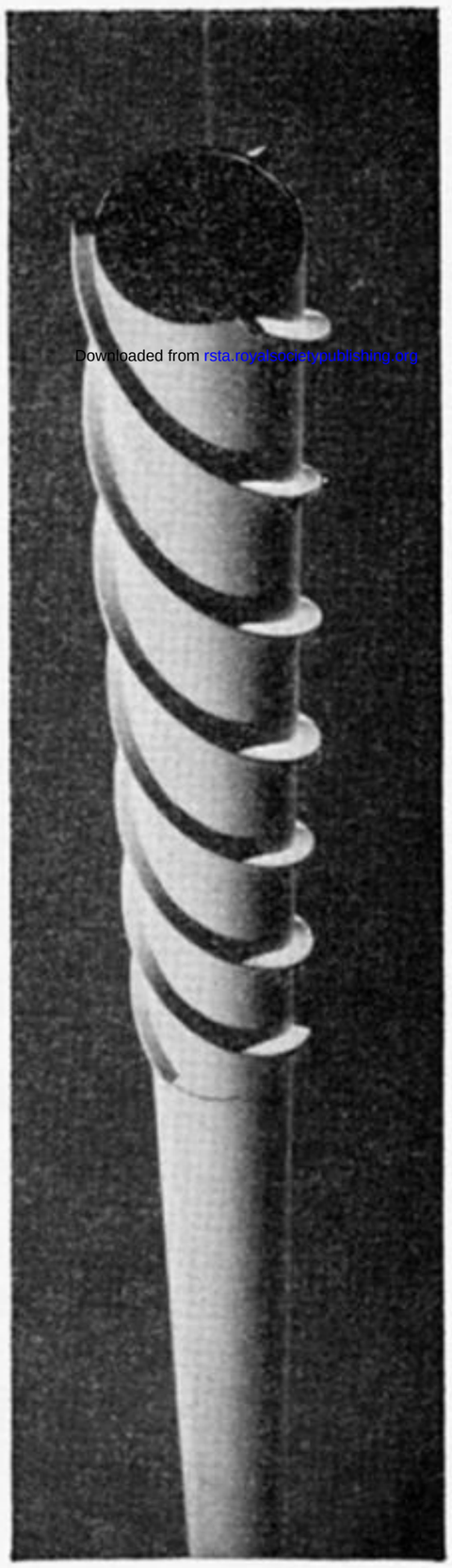

(a)

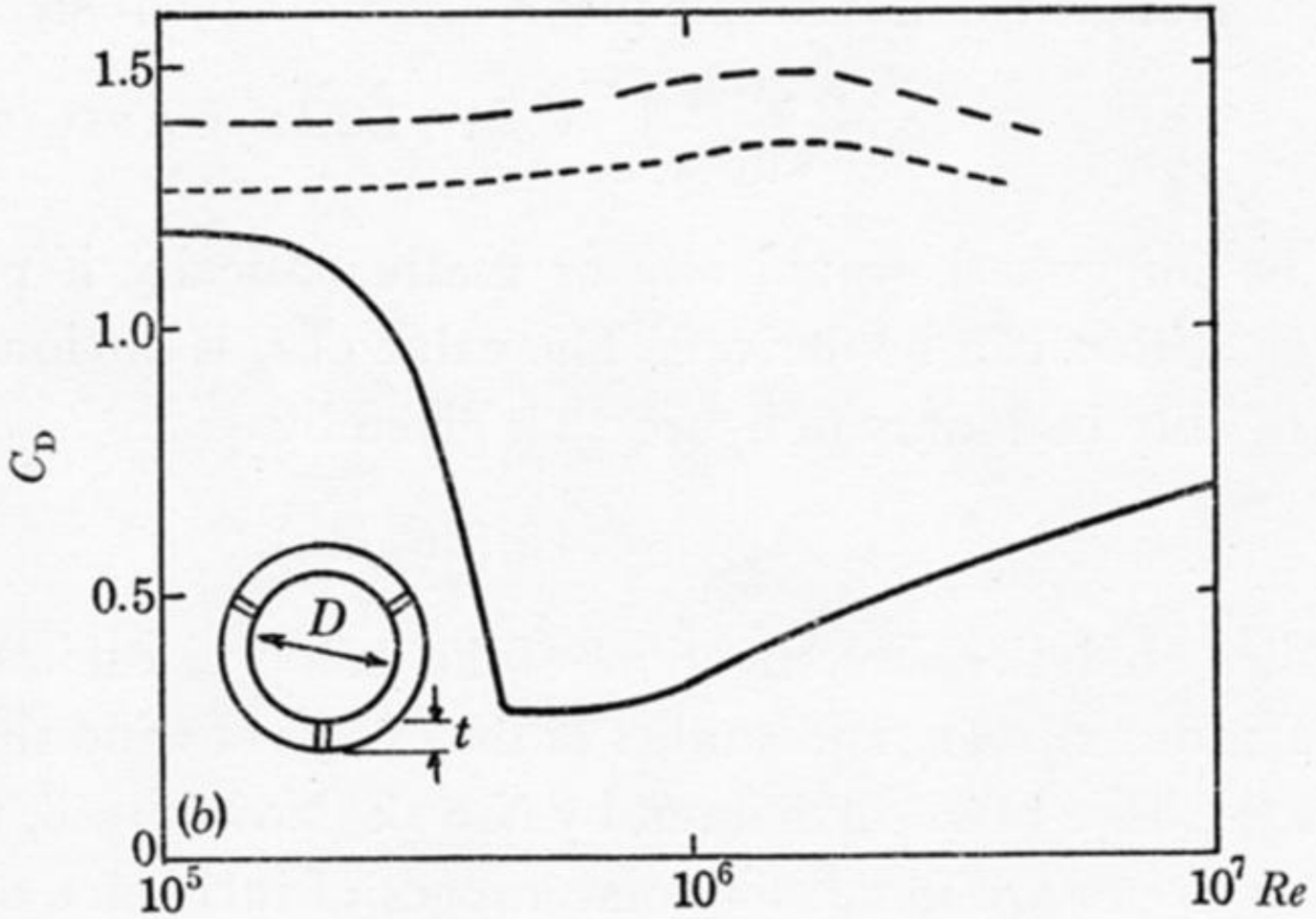

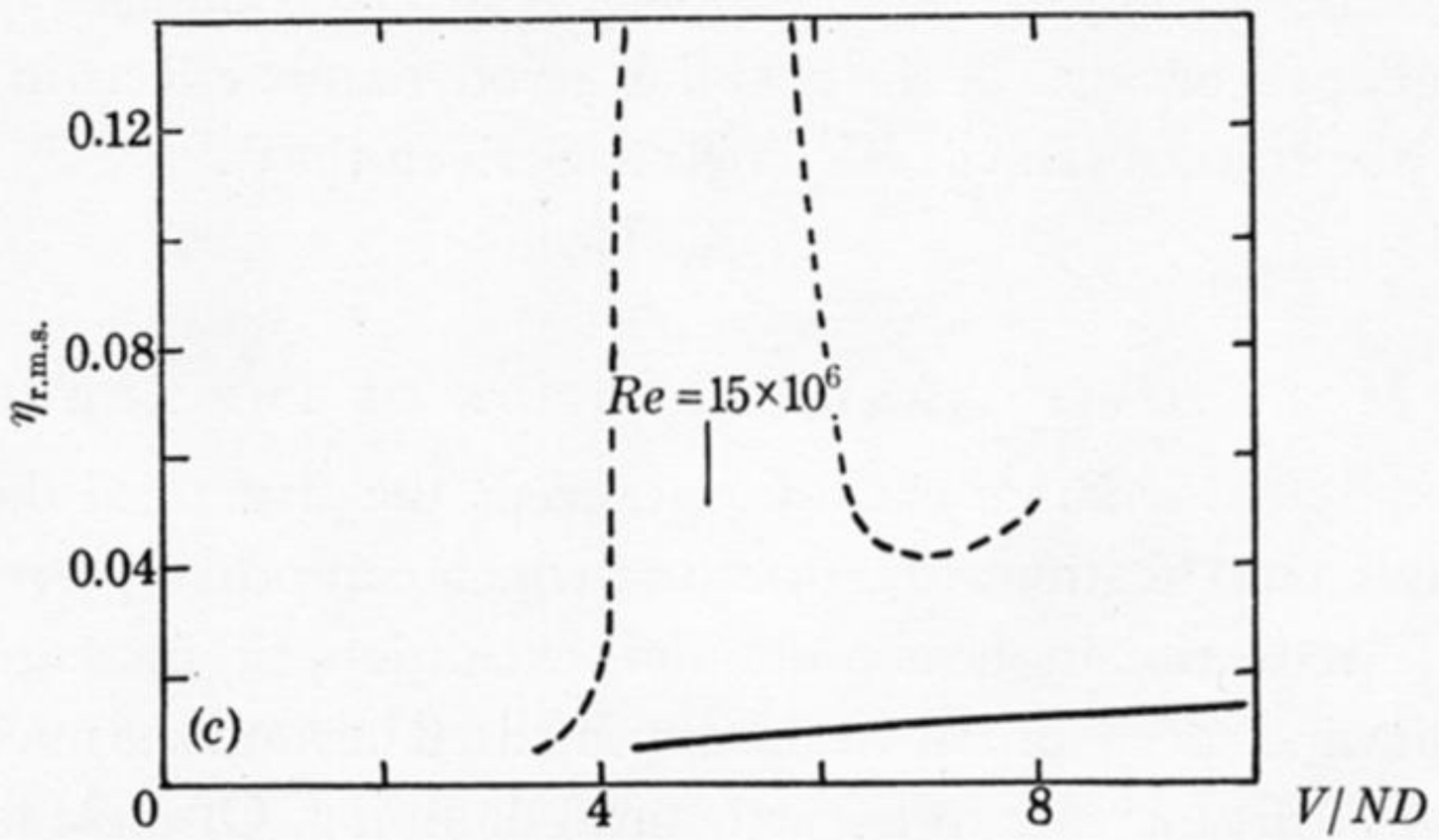

FIGURE 24. (*a*) A model straked stack. (*b*) The effect of Reynolds number on the drag coefficient of a plain straked circular cylinder. ——, plain cylinder; — — —, $t/D = 0.012$ and – – – –, $t/D = 0.006$ (cylinders with strakes). $C_D = D/\frac{1}{2}\rho V^2 DL$. (*c*) The responses of a model stack at high Reynolds numbers without and with strakes fitted over upper 30% of stack.

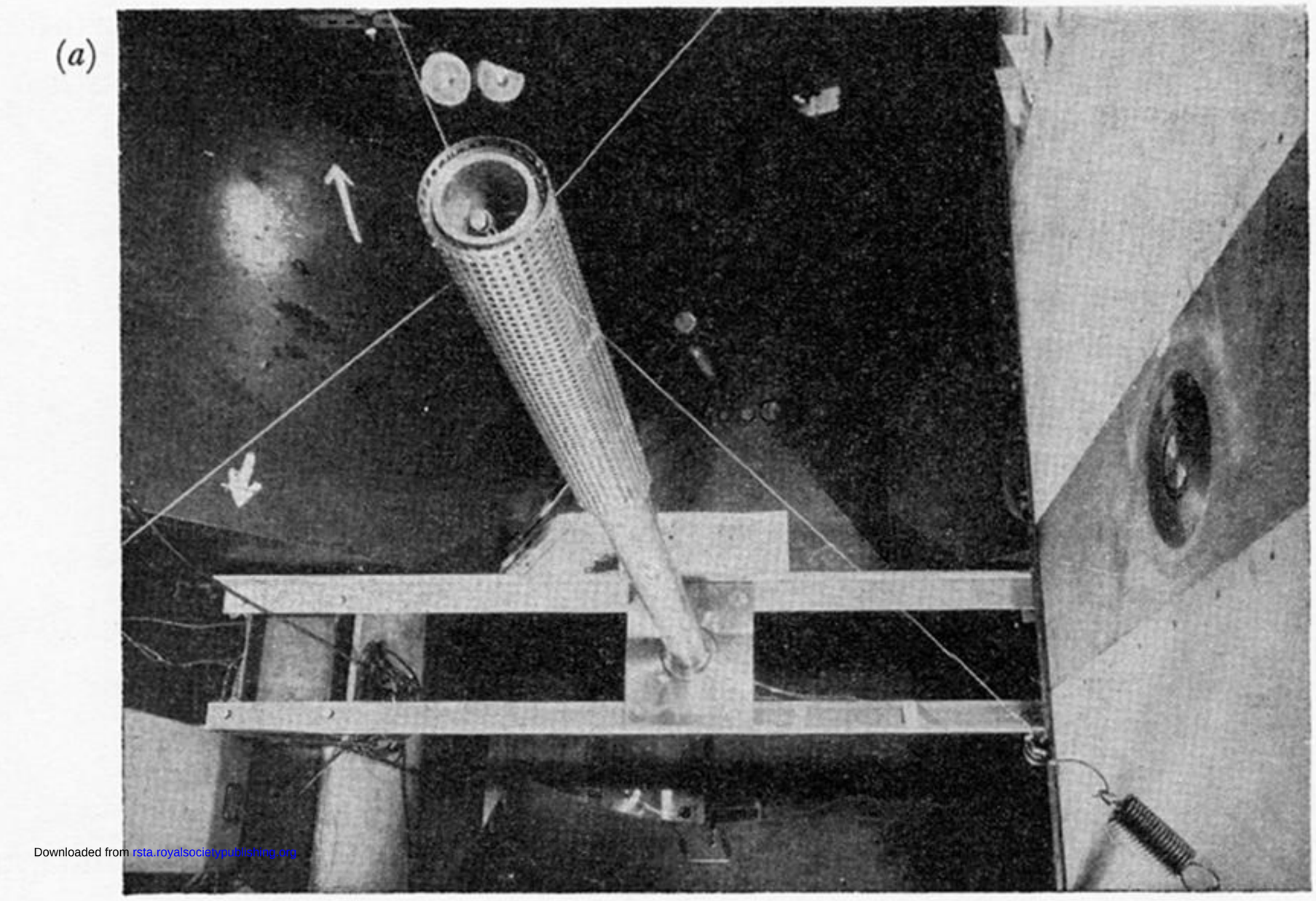

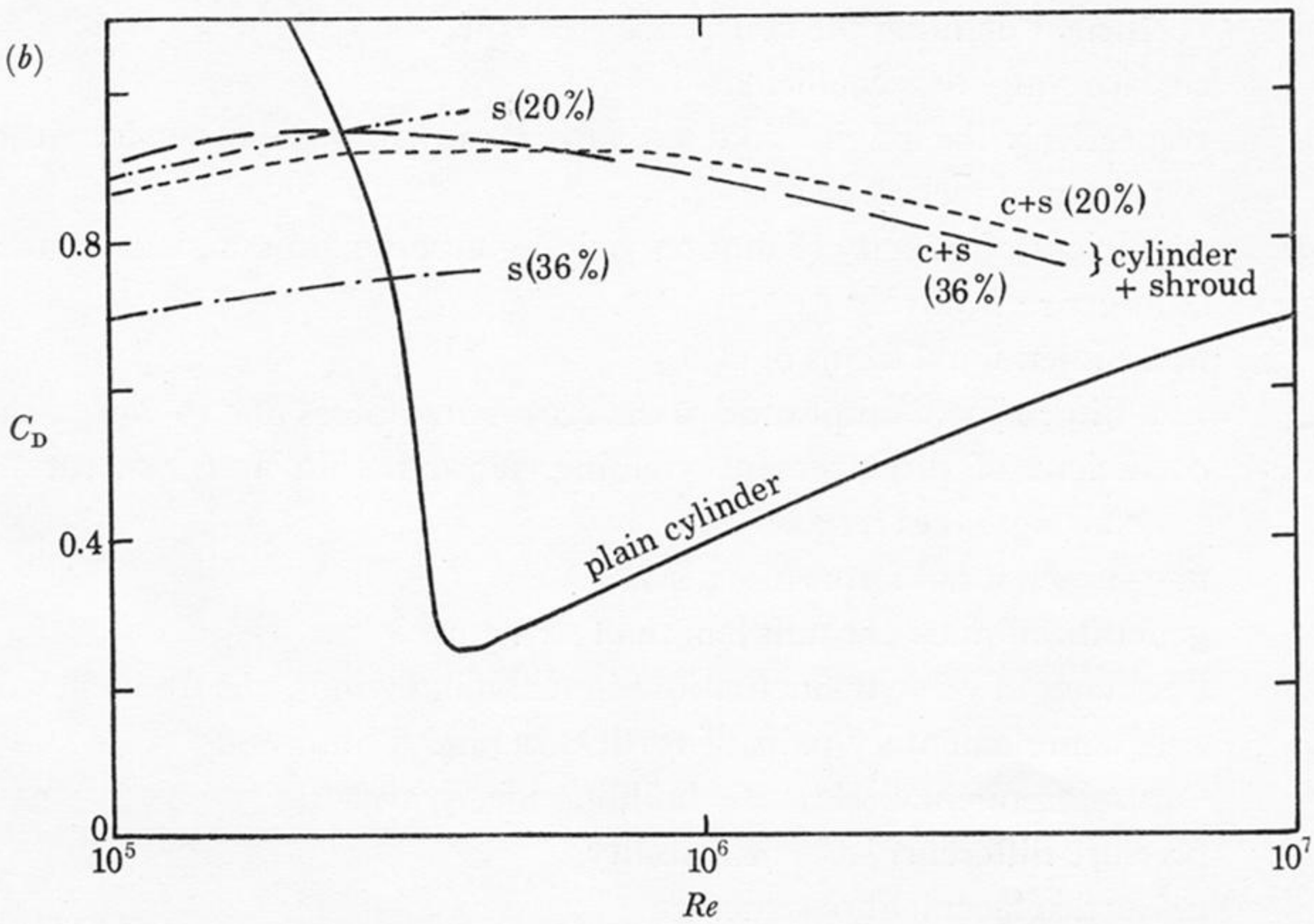

FIGURE 25. (*a*) A model shrouded stack. (*b*) The variation of drag with Reynolds number for a shrouded cylinder, shroud diameter/cylinder diameter = 1.23. *s*, shroud only; *c* + *s*, cylinder plus shroud. The percentages are the open ratios of the shrouds.

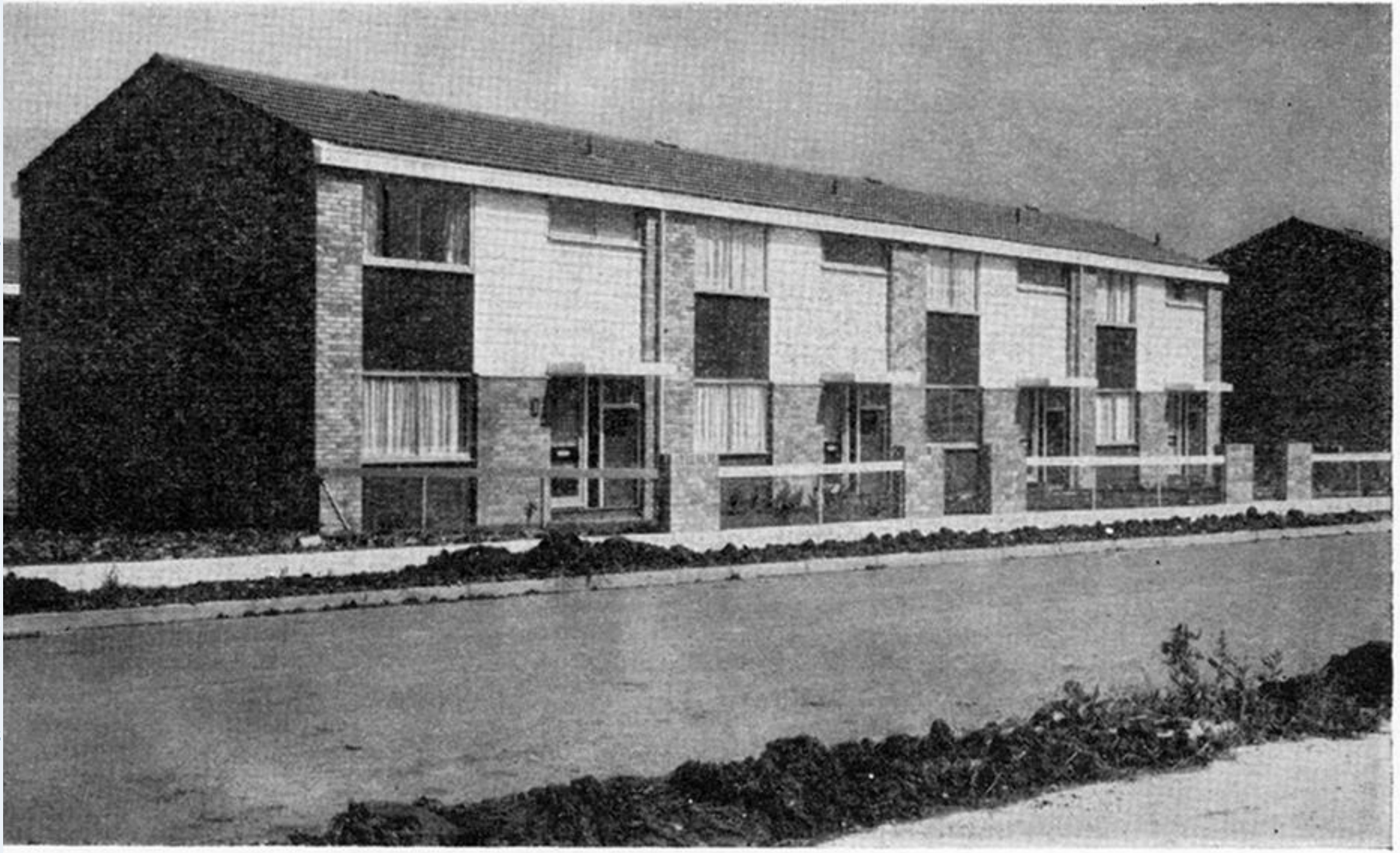

FIGURE 26

PHILOSOPHICAL TRANSACTIONS OF THE ROYAL SOCIETY A